

CHAPTER 3

MODELING AND ANALYSIS OF DIRECT AC-AC CONVERTERS FOR HIGH FREQUENCY APPLICATIONS

Contents

- 3.1 Introduction
- 3.2 High frequency Direct AC –AC converters:
 - 3.2.1 Three-phase to three phase HF generator:
 - 3.2.2 Three-phase to single-phase high frequency direct AC-AC converter
- 3.3 Simulation of the 3 Φ - 3 Φ high frequency direct AC-AC converter
- 3.4 The Proposed Converter & its Control
 - 3.4.1 Primary converter
 - 3.4.2 High frequency link transformer
 - 3.4.3 Secondary converter
- 3.5 Simulation of the Proposed Technique

Modeling and Analysis Direct AC-AC Converters for High Frequency Applications

3.1 Introduction:

Generation of electrical power to meet the increasing demands of the consumers and reduce T&D losses has always been a great question for all the nations across the world. This had led to some increase in the development of distributed power generation and storage technologies in over all generation. Also to avoid the dependency on the utilities for the electrical power as the single source and to achieve uninterrupted supply of electrical power, new commercial and residential schemes are coming forth with stand alone or distributed power sources. Most of the times, these sources are either micro turbines or wind turbines. All these energy technologies yield the electrical power that is incompatible with the requirements of the load and existing utility sources.

In the previous chapter, various topologies and performance of direct AC-AC converters for low frequency applications have been studied. This chapter investigates the performance of direct AC-AC converters for high frequency applications. The role of the high frequency link is analyzed as this high frequency link serves as galvanic isolation and as power conditioner for some typical applications. Detailed simulations have been carried out for various topologies and results show the usefulness of the topology.

Numerous advantages have been illustrated by use of high frequency link in field of static power conversion. Few of the advantages are enumerated below:

- **Reduction in size of magnetic used:**

It is well known that the power throughput density in the transformer is proportional to the operating frequency. Hence by increasing the

frequency, higher utilization of the magnetic core is achieved leading to reduction in transformer size. A power electronic transformer employing a high frequency ac link stage was proposed to reduce power transformer volume [1].

- **Elimination of bulky Energy storage components:**

Some of the processes are fed from the standard utility voltages such as 230V, 380V and 480V with fixed frequency and need voltage transformation to meet the process requirements at variable frequencies. Also electrical galvanic isolation between variable frequency source and utility is required for safety consideration. Conventional VSCF systems employ an AC to DC converter, dc-link, DC to AC inverter followed by a line frequency isolation transformer. Major disadvantage of this method is requirement of bulky 50 Hz magnetic components and large dc-link electrolytic capacitors [4], [5].

- **Capability to control independently real and reactive components of power**

It is possible to operate the converter at power factor of consumer requirement. Unity power factor operation is also possible during the conversion process.

- **Other advantages are**

- Bi-directional flow of power can be achieved.
- Electrical isolation achieved due to usage of transformer.
- Precise output voltage and input current wave shaping.
- Power density increased due to absence of low frequency filters and dc energy storage components.

Owing to these advantages, nowadays static converters with high frequency link are used for lightweight DC/AC converters [2] for UPS/inverter application and AC/DC conversion with zero-voltage switching [3] for high power rectifier. The proposed topology has many applications such as high frequency melting as both the features of small

size and high frequency output can be achieved with an added advantage of high quality input current waveform.

As mentioned earlier, energy crises all over the world has led to development of new energy technologies that yield output voltage and frequency that are incompatible with the existing utility in terms of grid pollution and interconnection has become a topic of greater concern for technologists. There arises a major role of static power converters, to be integrated with these technologies to provide the necessary compatibility. Although many attempts have been made and published but all the control algorithms are highly complex and difficult to understand. The static converter proposed here is also suitable for generation of fixed frequency output voltages from variable frequency source voltages.

The implementation of control algorithm for such converters was always a matter of concern for the researchers. A new three-phase AC/AC converter using high-frequency link converter with simple and robust control strategy is proposed in this chapter. The implementation is so simple that it can be achieved by using analog circuits. Digital ICs and DSP programming can be used for real time and precise control along with reduction in size of control cards. The principle used is similar to that of a single phase AC chopper. Major difference is that it has three phase inputs and generates in sequence 50% duty single-phase square wave pulses. The presence of multiphase inputs tends to increase the complexity of control. The single-phase high frequency pulses act as input to a transformer used to achieve the rated voltage level. These pulses are then rectified using an active full bridge diode rectifier. The output DC of the rectifier serves as an input to the inverter module generating the variable amplitude voltage at a desired frequency. This topology contains all the advantages of conventional AC-DC-AC converter along with an added advantage of elimination of DC components. Unity displacement factor is achieved at the input terminals.

3.2 High frequency Direct AC –AC converters:

In the earlier seventies, thyristors based technologies were mainly focused due to the availability of high power thyristors and their superior performance in high power applications. With the advancement of power semiconductors and development of transistors, GTOs, IGBTs and now MCTs, it has been proved that IGBTs are far most economical choice for many applications involving high frequency conversions. Integrated-insulated discrete components and also modules allow the implementation of the novel circuit topology with small and compact size. The generalized static converter topology can be readily used to synthesize high frequency multiphase/single phase output voltages from low frequency multiphase input. An illustration of three-phase to three-phase high frequency generator without galvanic isolation is modeled and analyzed in the following section.

3.2.1 Three-phase to three phase HF generator:

Figure 3.1 shows a three-phase to three-phase high frequency generator resulting from the generalized static converter structure by putting the number of input phases and number of output phases equal to three. In practice such a converter find applications where fixed utility supply is available and the user is in need of high frequency output voltages. The frequency range varies from several hertz to several kilohertz depending on the system requirements. Especially this is useful for military applications working on 400 Hz supply. Other applications may be typical high frequency loads such as high frequency welding applications etc.

The methods of control described in the previous chapter that is

- Direct Mode operation (DMO)
- Indirect mode operation (IMO)

are applicable to the high frequency direct AC-AC converter also.

The basic conversion equations for the output voltages and input current for both the control modes will remain the same as explained in chapter

II. If DMO is applied, the main advantage is the output to input voltage ratio achieve is maximum. But a disadvantage is the presence of high percentage of low order harmonics in the generated voltage waveforms. But it is noteworthy that the input current does not contain that high percentage of low order harmonics provided that $f_o \geq f_i$, where f_o is output frequency and f_i is the input frequency.

IMO is a two step process employing the conversion of input voltages to intermediate virtual DC voltage and then these DC voltage is converted in to high frequency voltages pulses at the output terminals of the converter.

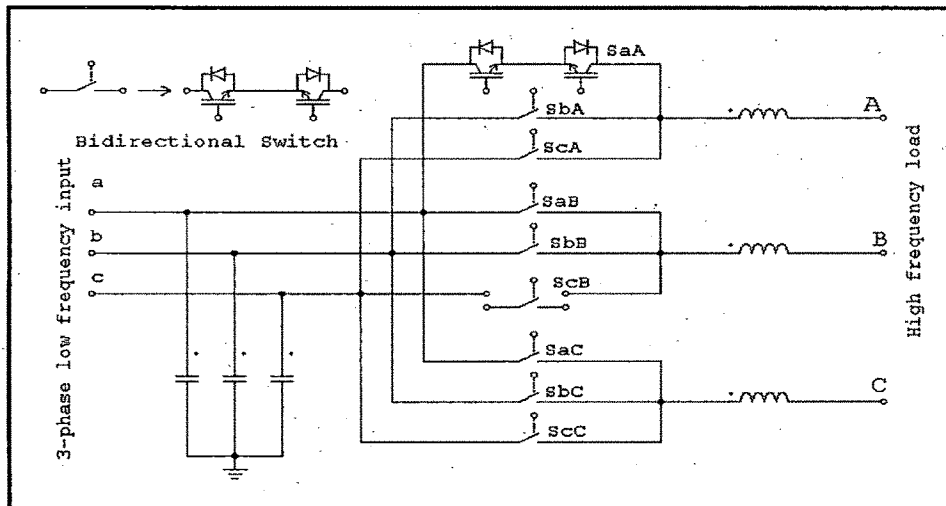


Fig 3.1 Three-phase to three-phase high frequency generator

3.2.2 Three-phase to single-phase high frequency direct AC-AC converter

Three-phase to single phase high frequency converter can be realized by following two configurations:

- Half bridge configuration (4 switch) and
- Full bridge configuration (6 switch)

Half bridge configuration is realized by usage of four bidirectional switches; three switches connected to each phase and fourth switch connected to neutral as shown in figure 3.2 below:

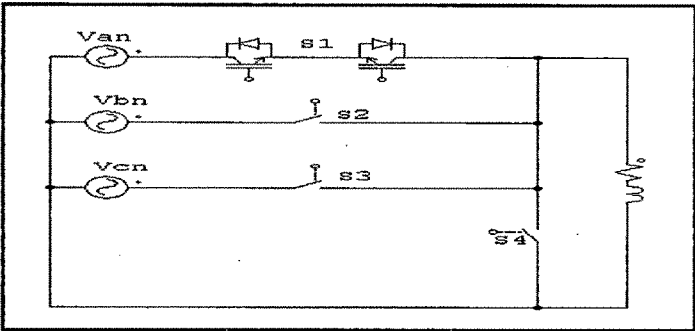


Fig 3.2 Simplified power circuit diagram for the three-phase to single-phase direct high frequency AC-AC converter (half bridge configuration)

This topology is particularly useful where the neutral connection at the source terminals is available i.e. three phase four wire systems. Only the direct mode operation control technique can be employed due to half bridge configuration of power circuit used.

Full bridge configuration (fig 3.3) is realized by using the generalized structure of Direct AC-AC converter, explained in chapter II by setting number of input phases $M=3$ and number of output phases $N=1$.

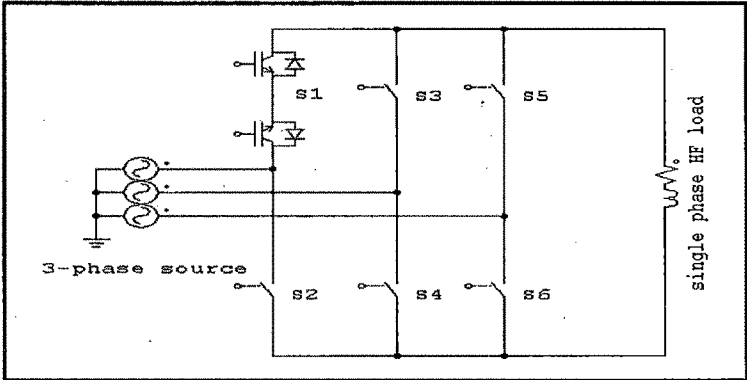


Fig 3.3 Simplified power circuit diagram for the three-phase to single-phase direct high frequency AC-AC converter (full bridge configuration)

The application of this topology is more appropriate to AC/DC power conversion process viz. switch mode power supplies; wherein there is a usage of high frequency ohmic isolation. Both the modes of operation i.e. DMO and IMO can be employed to generate the desired output.

3.3 Simulation of the 3 Φ - 3 Φ high frequency direct AC-AC converter

Direct mode operation is used for generating the high frequency voltages across the load. Detailed simulation has been carried out for three-phase to three-phase high frequency converter.

Simulation Parameters:

System parameters:

Case I

Input voltage: 415 Volts, 3-phase

Input frequency: 50 Hz

Output voltage: User selectable (0-400 volts range)

Output frequency: 400 Hz

Output load parameters: R= 10 ohms, L = 19 mH

Explanation: In the simulation model, the 9 switch topology is used to generate the high frequency voltages aiming the defense as an end application from a variable frequency input source. Further the same can be extended for using for heating applications also. Waveforms shown indicate that the input currents are quite sinusoidal with high frequency glitches which can be easily filtered. The output waveform is a combined waveform of having two distinct frequency components one is the 6th harmonic component and other is the high frequency switching component.

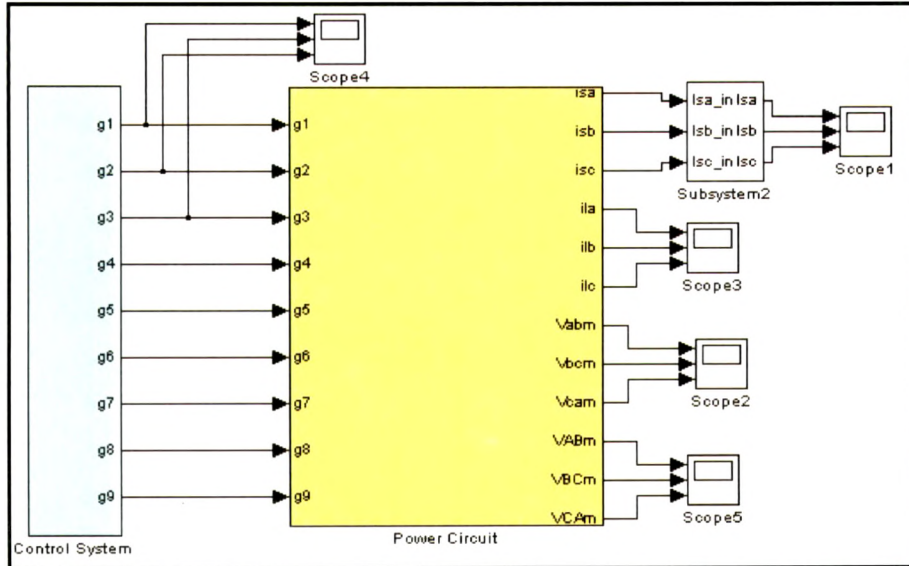


Fig S_{3.1} Simulation block diagram of three-phase to three-phase high frequency generator

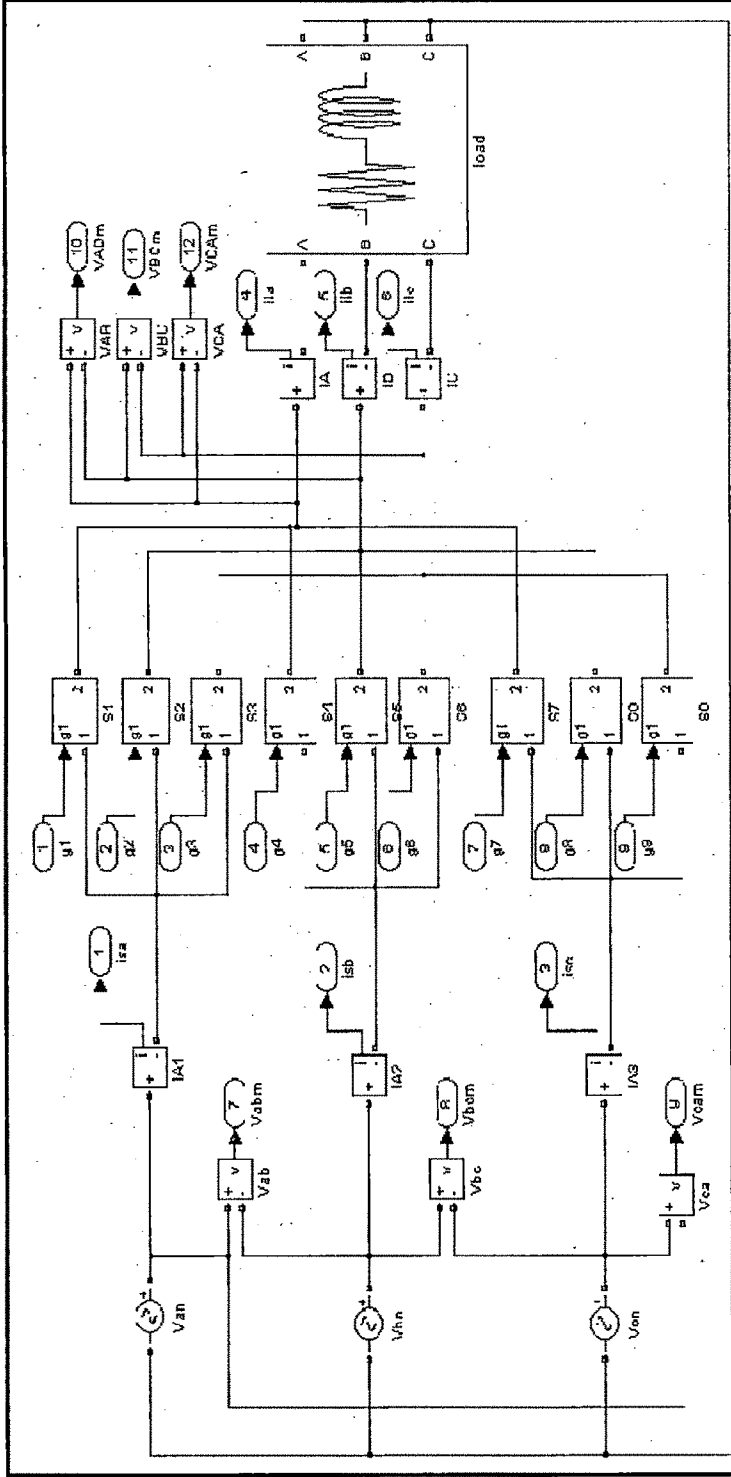
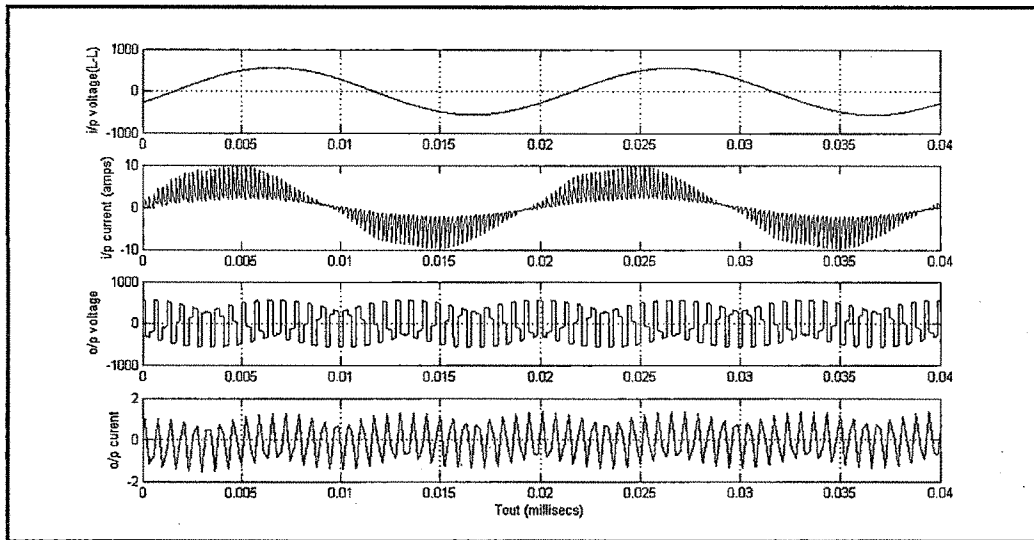


Fig S3.2 Simulation Power Circuit of three-phase to three-phase high frequency generator



**Fig. S_{3.3} Input voltage (L-L)
Input current
Output voltage
Output current at RL load**

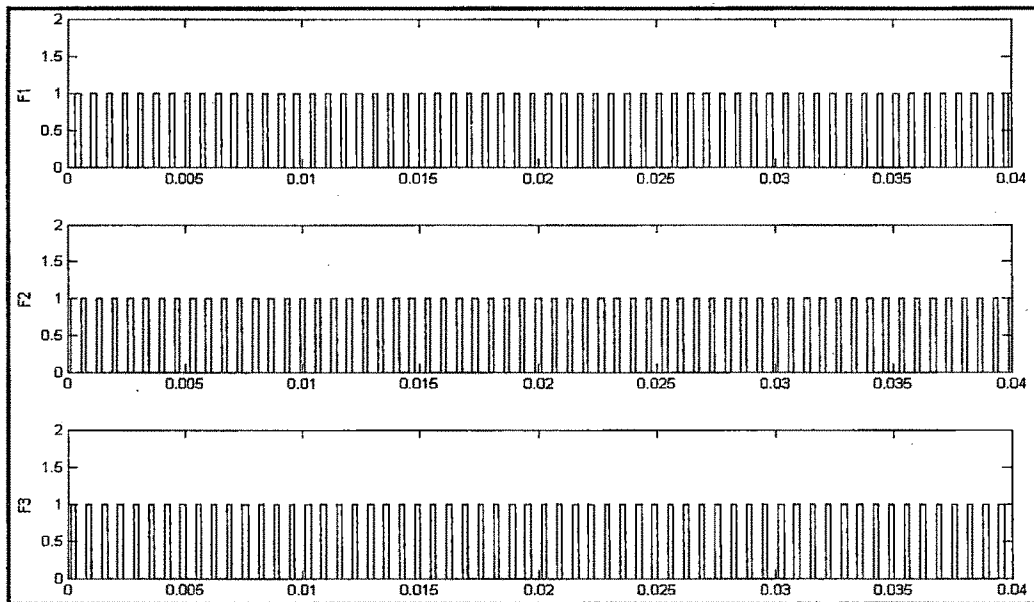


Fig. S_{3.4} Waveforms of the switching functions F₁, F₂ & F₃

3.4 The Proposed Converter & its Control

The proposed high frequency link converter topology consists of following two power conversion stages :

- PRIMARY CONVERTER: Fixed frequency utility supplied multiphase to high frequency single-phase converter.
- SECONDARY CONVERTER: The consumer suitable single-phase to three phase variable voltage, variable frequency converter.

Basically primary converter is a three-phase to single-phase high frequency converter. It employs six bidirectional switches for conversion of low frequency balanced three phase utility supply voltages to 50% duty cycle high frequency square wave pulse. Secondary converter also uses six bidirectional switches to convert the high frequency voltages to three-phase low frequency output. High frequency transformer is used as an intermediate link between the above-mentioned converters. This high frequency transformer is fed with high frequency AC square wave pulses. High frequency transformer serves two purposes; firstly it provides electrical galvanic isolation and secondly user defined output voltage transfer ratio can be achieved by using appropriate turns ratio.

3.4.1 Primary converter

A simple and robust control technique based on detection of maximum conducting phase voltage is applied and it is also ensured that 50% duty cycle of square waves is maintained throughout. Each bi directional switch is modeled by using the two IGBTs connected in series in common emitter configuration with diodes in anti-parallel as shown in figure 3.4 below.

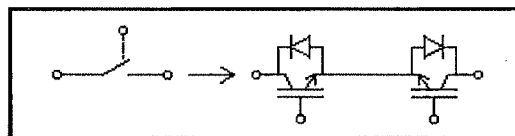


Fig 3.4 Modeling of bidirectional switch using two IGBTs with two anti-parallel diodes

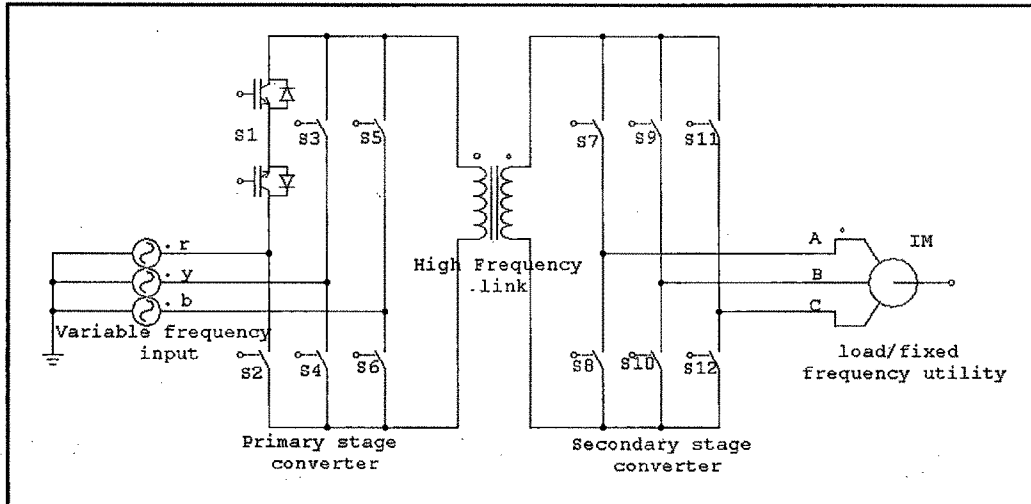
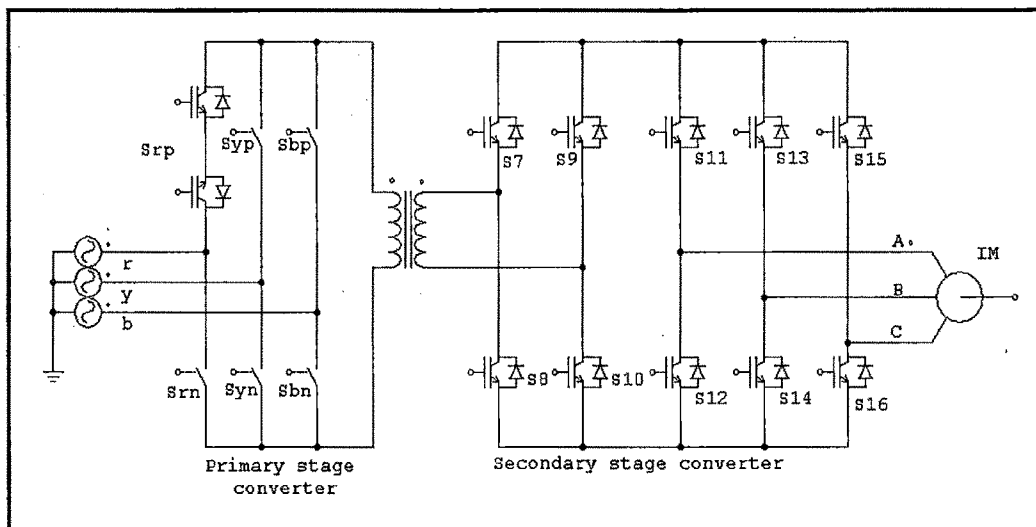


Fig 3.5 The proposed Direct AC-AC high frequency link converter.

In the proposed technique, to understand and implement the primary and secondary converters for simplifying the analysis, the secondary converter is modified and instead of six bidirectional switches, ten unidirectional semiconductor switches are used as shown in figure 3.6 below. This modification makes the study of behavior of converter simpler and easy.



Out of these ten unidirectional switches, four are used to rectify the high frequency voltage to unfiltered DC voltage. S₇-S₁₀ form a full bridge rectifier and S₁₁-S₁₆ form an inverter, which generates the low frequency voltages of desired amplitude and arbitrary frequency. The control algorithms for three phase inverters are well known to all and easy to implement. Suitable algorithm can be applied so that the output voltages have less content of harmonics and high efficiency of the converter is ensured. The magnitude of the DC voltage can be achieved by appropriate design of the high frequency transformer having transformation ratio of 1: n or having a tapped secondary transformer for more general use.

Analysis of Primary converter

As mentioned earlier this primary converter is used to convert the utility supplied three-phase supply voltage having fixed frequency to high frequency pulses. This is achieved by chopping the input voltages in a predetermined manner. The control method applied is based on detection of maximum conducting phase for generation of modulation signal. Consider the following balanced set of three phase input voltages as shown in figure 3.7 below:

$$V_r = V_m \sin(2\pi f_{in} t) \quad (3.1.a)$$

$$V_y = V_m \sin\left(2\pi f_{in} t - \frac{2\pi}{3}\right) \quad (3.1.b)$$

$$V_b = V_m \sin\left(2\pi f_{in} t - \frac{4\pi}{3}\right) \quad (3.1.c)$$

Where V_m is the maximum value of the input phase voltage
 f_{in} is the supply frequency of the source

Initially study the three phase waveforms for one complete cycle of 360 degrees for any phase as a reference. Three phase waveforms can be divided into six sectors corresponding to period of time (as one sector) of

the consecutive two zero crossings of the signals (refer fig. 3.7). Each period is of sixty degrees if it is defined in term of 360 degrees per cycle.

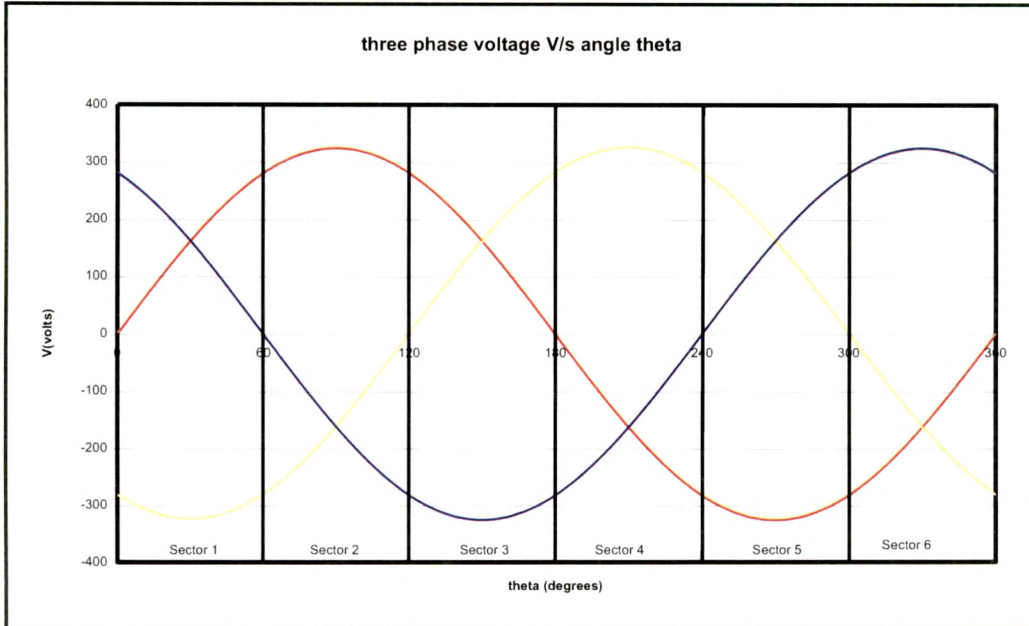


Fig 3.7 Waveforms of input phase voltages and its division into six sectors

Observing each period of sixty degrees, it can be seen that during each period one of the phase attains maximum absolute value and the other phases have the magnitude of opposite polarity. Refer to the figure 3.7. It can be seen that for a period of sixty degrees from zero of R-phase to zero crossing of B-phase, the magnitude of Y-phase voltage attains maximum value in negative cycle and the R-phase and B-phase voltages are having positive magnitudes. For the sake of simplicity, we identify this period of 60° as sector I. For a balanced set of three phase voltages, it is well known that algebraic sum of instantaneous values of three phase voltages is zero. For this sector also it holds true, i.e.

$$\boxed{|V_y| = |V_r| + |V_b|} \quad (3.2)$$

Selection of the sequence of conducting switches depends on the magnitude of the RMS values of square pulsed voltages to be generated. Let us consider that maximum possible voltages are to be generated

across the high frequency transformer. For sector I, it can be said that the maximum voltages can be generated by following combinations of voltages.

$$V_b-V_y \text{ \& } V_r-V_y$$

Thus from the above relation we can see that V_y is common in both the relations meaning that the y phase remains on or connected throughout the period of these sixty degrees, while the other two phases can be modulated as per the requirements. Thus the whole cycle process (for all sectors from Sector 1 to 6) can be summarized in the following table 3.1.

Table 3.1 Selection of sector and corresponding phase switches

Sr. No	Sector No.	Switching sequence		Voltages generated	
		Phase continuously conducting for 60°	Modulating phases		Total voltage generated in each interval
1)	1	-Y phase	+B phase	V_b-V_y	$(V_b-V_y) +$
			+R phase	V_r-V_y	(V_r-V_y)
2)	2	+R phase	-Y phase	V_r-V_y	$(V_r-V_y) +$
			-B phase	V_r-V_b	(V_r-V_b)
3)	3	-B phase	+R phase	V_r-V_b	$(V_r-V_b) +$
			+Y phase	V_y-V_b	(V_y-V_b)
4)	4	+Y phase	-B phase	V_y-V_b	$(V_y-V_b) +$
			-R phase	V_y-V_r	(V_y-V_r)
5)	5	-R phase	+Y phase	V_y-V_r	$(V_y-V_r) +$
			+B phase	V_b-V_r	(V_b-V_r)
6)	6	+B phase	-R phase	V_b-V_r	$(V_b-V_r) +$
			-Y phase	V_b-V_y	(V_b-V_y)

Once the identification of appropriate phases is completed, the duty cycle calculation for each switch is required to be carried out for calculating the switching time for all the switches. As shown in figure 3.5, each leg of the primary converter contains two bidirectional switches and each bidirectional switch contains two IGBT switches connected in common emitter mode (fig 3.4). Consider the switching time period of T_{sw} for generation of high frequency pulses having the frequency of F_{sw} . For calculating the duty ratio for each bidirectional switch, it is necessary to determine the maximum contributing phase. Calculating the maximum value of the instantaneous absolute values of input voltages will identify the maximum contributing phase. Once the maximum value is calculated, the duty cycle can be calculated by dividing the absolute value of each phase voltage by the maximum absolute voltages as shown in equations below.

$$d_r = \frac{|\sin(\omega_r t)|}{\max(|\sin \omega_r t, \sin(\omega_r t - 2\pi/3), \sin(\omega_r t - 4\pi/3)|)} \quad (3.3.a)$$

$$d_r = \frac{|\sin(\omega_r t - 2\pi/3)|}{\max(|\sin \omega_r t, \sin(\omega_r t - 2\pi/3), \sin(\omega_r t - 4\pi/3)|)} \quad (3.3.b)$$

$$d_r = \frac{|\sin(\omega_r t - 4\pi/3)|}{\max(|\sin \omega_r t, \sin(\omega_r t - 2\pi/3), \sin(\omega_r t - 4\pi/3)|)} \quad (3.3.c)$$

If we consider a small period of time $t=T_{sw}$ and if we are in sector 1, then the value of d_y will be equal to one for the time period of T_{sw} and also throughout the interval of 60° while the value of d_r will be line having positive slope starting from 0 till it reaches the value of 1 and d_b will be line having negative slope starting from 1 till it reaches the value of 0.

Now in the sector 1, for constructing the positive pulse across the transformer switch S_{yn} is turned on for the period of $T_{sw}/2$, while S_{bp} and S_{rp} are modulated, while all other switches remain off.

Negative part of the high frequency wave is generated by forcing the S_{yn} to off condition and turning on S_{yp} for a period of $T_{sw}/2$. The switches S_{bn}

and S_{rn} are modulated for this period of $T_{sw}/2$. The mechanism of generation of square pulses is explained in detailed in the following section.

Hence this converter can be considered as a forced commutated cyclo-converter and its implementation is possible due to availability of semiconductors as IGBTs, MCTs etc.

Mechanism for generation of high frequency wave:

As explained above, it is clear that the positive cycle has combination of two pulses. One part is generated due to conduction of S_{yn} and S_{bp} for a part (i.e. duty cycle db) of time period $T_{sw}/2$ and the circuit is completed through these switches connecting phase Y to phase B and the high frequency transformer as shown in figure 3.8.

When S_{bp} is turned off depending on the modulation principle, S_{yn} is still conducting. At this instant S_{rp} is turned on for the remaining part (i.e. duty cycle dr) of $T_{sw}/2$ and the circuit is now completed through S_{yn} , high frequency transformer and S_{rp} (refer fig 3.9). These two sequences of switching contribute to formation of positive pulse. Thus it can be said that a pulse of current initially flows from phase B to phase Y and then phase R to phase Y. This forms total positive current pulse flowing through high frequency transformer

To maintain the flux balance and to avoid the saturation of the high frequency transformer, it is necessary to apply a negative voltage pulse to the transformer during the remaining $T_{sw}/2$ part of the period immediately after positive pulse. For applying a negative pulse, S_{yp} is turned on for the time period of $T_{sw}/2$. The switches S_{bn} and S_{rn} are modulated similar to that done in case of generation of positive pulse. Here a negative voltage pulse is applied by turning on S_{yp} and S_{bn} , connecting the B phase to the Y phase through the high frequency transformer (fig 3.10).

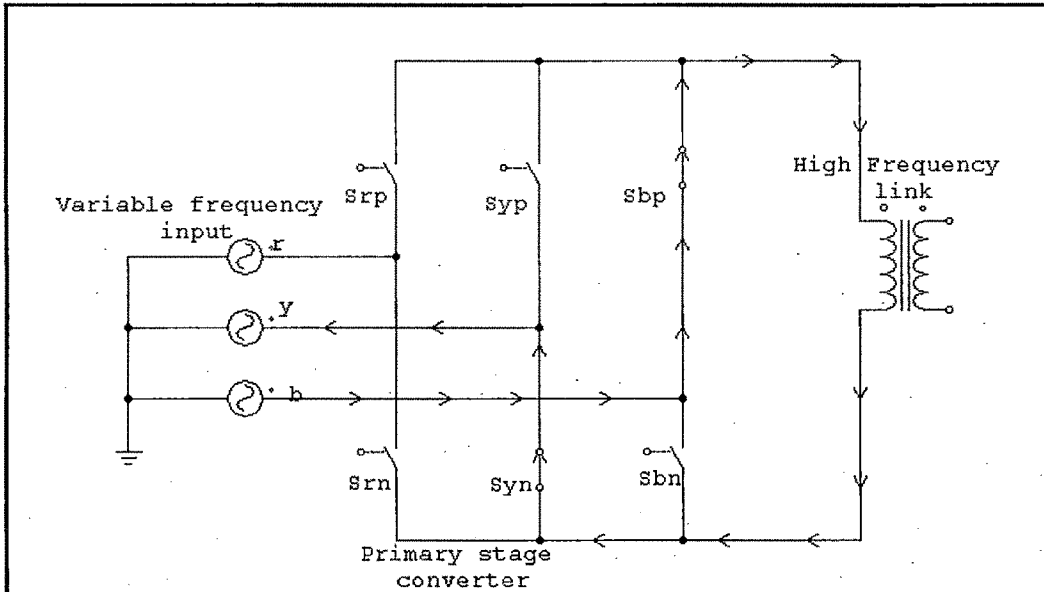


Fig 3.8 Equivalent circuit diagram for sector one when S_{yn} & S_{bp} are conducting

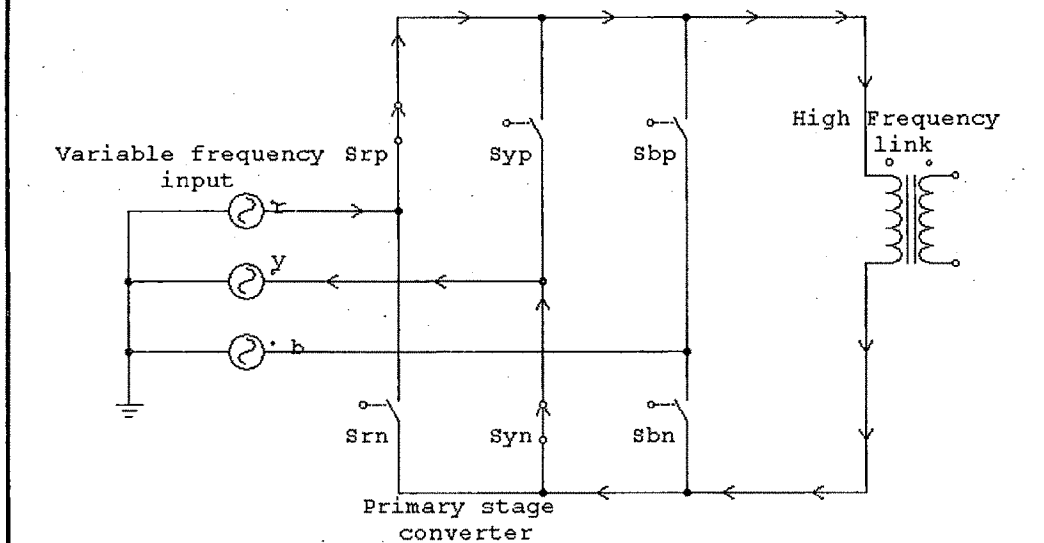


Fig 3.9 Equivalent circuit diagram for sector one when S_{yn} & S_{rp} are conducting

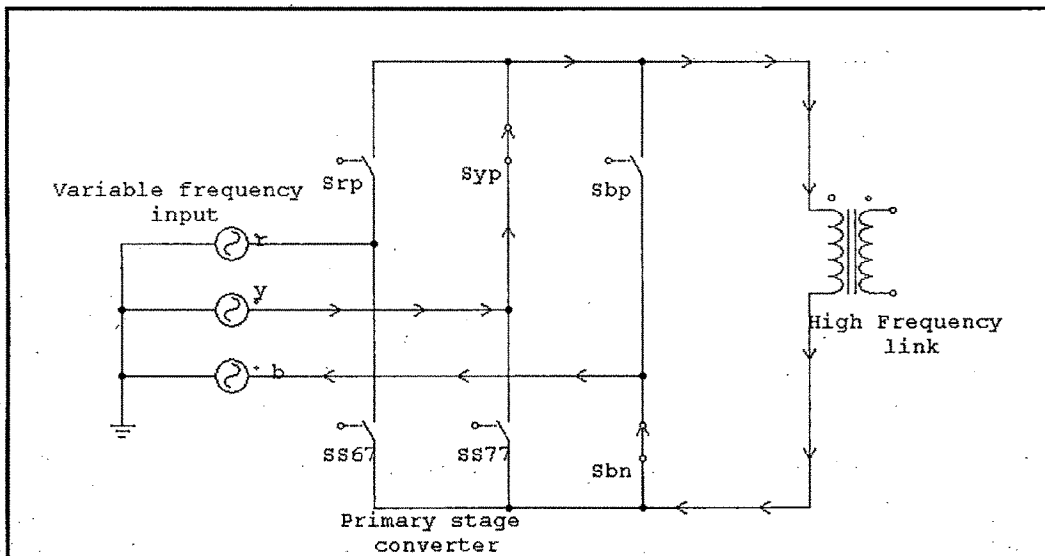


Fig 3.10 Equivalent circuit diagram for sector one when S_{yp} & S_{bn} are conducting

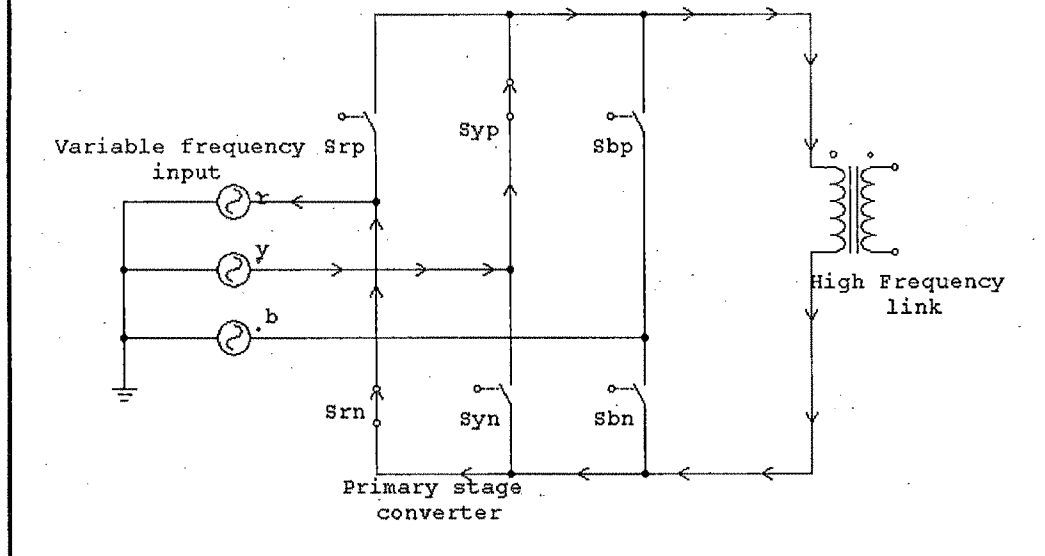


Fig 3.11 Equivalent circuit diagram for sector one when S_{yp} & S_{rn} are conducting

Then S_{bn} is switched off and S_{rn} is turned on and S_{yp} continues to be on connecting R phase to Y phase. This sequence is continued up to completion of sector 1 i.e. sixty degrees and then in sector 2, the role of

switches change maintaining 50 % duty cycle through the period (fig 3.11).

50% duty cycle square pulses are assured in this case because the input voltages are assumed to be balanced and are sampled at a high frequency. So always the magnitude of the voltages across the terminals i.e $[(V_b - V_y) + (V_r - V_y)]$ during the one time interval of $T_{sw}/2$ will be equal to succeeding time interval of $T_{sw}/2$.

This pulsed voltage then can be converted to required magnitude by stepping up/down or providing tapping on secondary side of transformer. High frequency positive and negative ramps are used to generate gate pulses for each bi-directional switch, Ramp signals helps the designer in maintaining 50 % width pulses.

3.4.2 High frequency link transformer

A transformer is based on two principles: firstly, that an electric current can produce a magnetic field (i.e. electromagnetism) and secondly that a changing magnetic field within a coil of wire induces a voltage across the ends of the coil (electro magnetic induction). Changing the current in the primary coil changes the magnitude of the applied magnetic field. The changing magnetic flux extends to the secondary coil where a voltage is induced across its ends. A simplified transformer design is shown in the figure 3.11 below. A current passing through the primary coil creates a magnetic field. The primary and secondary coils are wrapped around a core of very high magnetic permeability, such as iron; this ensures that most of the magnetic field lines produced by the primary current are within the iron and pass through the secondary coil as well as the primary coil. The voltage induced across the secondary coil may be calculated from Faraday's law of induction, which states that:

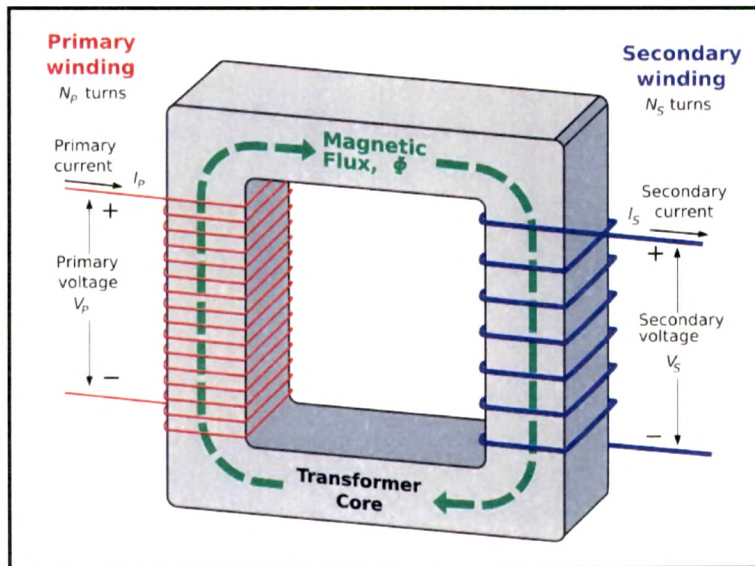


Fig. 3.12 A simplified transformer design

$$V_S = N_S \frac{d\phi}{dt} \quad (3.4)$$

where V_S is the instantaneous voltage, N_S is the number of turns in the secondary coil and Φ equals the magnetic flux through one turn of the coil. If the turns of the coil are oriented perpendicular to the magnetic field lines, the flux is the product of the magnetic field strength B and the area A through which it cuts. The area is constant, being equal to the cross-sectional area of the transformer core, whereas the magnetic field varies with time according to the excitation of the primary. Since the same magnetic flux passes through both the primary and secondary coils in an ideal transformer, the instantaneous voltage across the primary winding equals

$$V_P = N_P \frac{d\phi}{dt} \quad (3.5)$$

Taking the ratio of the two equations for V_S and V_P gives the basic equation for stepping up or stepping down the voltage

$$\frac{V_S}{V_P} = \frac{N_S}{N_P} \quad (3.6)$$

Ideal power equation

If the secondary coil is attached to a load that allows current to flow, electrical power is transmitted from the primary circuit to the secondary circuit. Ideally, the transformer is perfectly efficient; all the incoming energy is transformed from the primary circuit to the magnetic field and into the secondary circuit. If this condition is met, the incoming electric power must equal the outgoing power.

$$P_{\text{incoming}} = I_P V_P = P_{\text{outgoing}} = I_S V_S \quad (3.7)$$

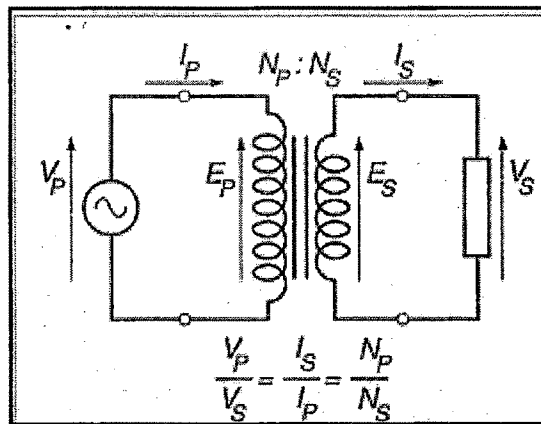
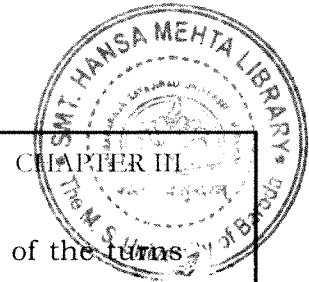


Fig 3.13 The ideal transformer as a circuit element

giving the ideal transformer equation

$$\frac{V_S}{V_P} = \frac{N_S}{N_P} = \frac{I_P}{I_S} \quad (3.8)$$

If the voltage is increased (stepped up) ($V_S > V_P$), then the current is decreased (stepped down) ($I_S < I_P$) by the same factor. Transformers are efficient so this formula is a reasonable approximation.



The impedance in one circuit is transformed by the *square* of the turns ratio. For example, if an impedance Z_S is attached across the terminals of the secondary coil, it appears to the primary circuit to have an

impedance of $Z_P \left(\frac{N_P}{N_S} \right)^2$

This relationship is reciprocal, so that the impedance Z_P of the primary

circuit appears to the secondary to be $Z_P \left(\frac{N_S}{N_P} \right)^2$

If the flux in the core is sinusoidal, the relationship for either winding between its rms Voltage of the winding E , and the supply frequency f , number of turns N , core cross-sectional area a and peak magnetic flux density B is given by the universal EMF equation

$$E = \frac{2\pi f N a B}{\sqrt{2}} \approx 4.44 f N a B \quad (3.9)$$

The time-derivative term in Faraday's Law shows that the flux in the core is the integral of the applied voltage. Hypothetically an ideal transformer would work with direct-current excitation, with the core flux increasing linearly with time. In practice, the flux would rise to the point where magnetic saturation of the core occurred, causing a huge increase in the magnetizing current and overheating the transformer. All practical transformers must therefore operate only with alternating (or pulsed) current. The EMF of a transformer at a given flux density increases with frequency. By operating at higher frequencies, transformers can be physically more compact because a given core is able to transfer more power without reaching saturation, and fewer turns are needed to achieve the same impedance. However properties such as core loss and conductor skin effect also increase with frequency. Aircraft and military

equipment employ 400 Hz power supplies which reduce core and winding weight.

From fig 3.5, it can be seen that the high frequency transformer can be viewed as a connecting link between two independent sources (if the output of the proposed converter is a fixed frequency utility source). The direction of power flow in such a case depends on the voltage magnitudes of both the sources and their corresponding phase angles.

3.4.3 Secondary converter

The main purpose of this converter is to provide a three-phase voltage source, where the amplitude, phase, and frequency of the voltages should always be controllable. As mentioned earlier, to make the operation of this converter simple i.e. conversion of high frequency pulses to three phase low frequency voltages, the converter is divided in two parts. Basically the converter, having six bidirectional switches (fig 3.5) is modified in two-stage converters, one is a single-phase full bridge converter and a three-phase full bridge inverter. Both the power converters are realized using unidirectional IGBTs with anti parallel diodes (fig 3.5). To achieve this objective, it is required to first convert the high frequency square waves into a DC voltage using a high frequency bridge rectifier. If the four-quadrant operation is not required then high frequency diode bridge is used in place of IGBT bridge rectifier. Output dc voltage is equated as

$$V_{dc} = n(d_b(V_y - V_b) + d_r(V_y - V_r)) \quad (3.10)$$

Where $n = \frac{\text{No of sec. turns}}{\text{No of pri. turns}}$, is the transformer turns ratio.

Once the DC output voltage is generated, it is required to convert this variable amplitude DC voltage into AC Voltages with arbitrary amplitude

and unrestricted frequency of three phase voltages to serve as a source to load.

Although most of the applications require sinusoidal voltage waveforms (e.g. ASDs, UPSs, FACTS, VAR compensators), arbitrary voltages are also required in some emerging applications (e.g. active filters, voltage compensators). The standard three-phase VSI topology is shown in Fig. - 3.14 and the eight valid switch states are given in Table 3.2.

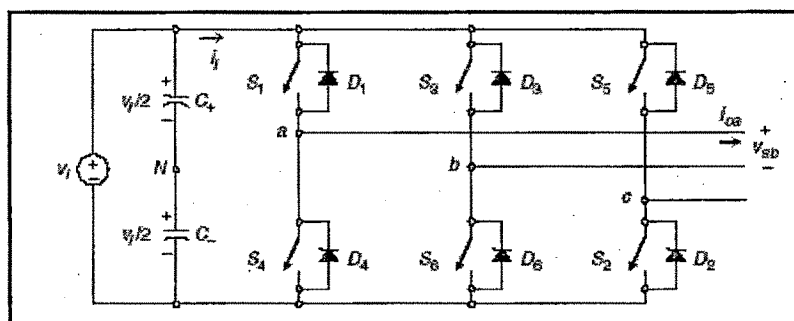


Fig 3.14 Three-phase inverter circuit

In case of three phase inverters, the switches of any leg of the inverter (S_1 and S_4 , S_3 and S_6 , or S_5 and S_2) cannot be switched on simultaneously because this would result in a short circuit across the dc link voltage supply. Similarly, in order to avoid undefined states in the VSI, and thus undefined ac output line voltages, the switches of any leg of the inverter cannot be switched off simultaneously as this will result in voltages that will depend upon the respective line current polarity. Of the eight valid states, two of them (7 and 8 in Table 3.2) produce zero ac line voltages. In this case, the ac line currents freewheel through either the upper or lower components.

The remaining states (1 to 6 in Table 3.2) produce non-zero ac output voltages. In order to generate a given voltage waveform, the inverter moves from one state to another.

Thus the resulting ac output line voltages consist of discrete values of voltages that are v_i , 0, and $-v_i$ for the topology shown in fig 3.15. The selection of the states in order to generate the given waveform is done by

the modulating technique that should ensure the use of only the valid states.

Table: 3.2 Switching States and Switch Condition for three-phase inverter

Switch Condition	State No	V_{ab}	V_{bc}	V_{ca}
$S_1, S_2,$ and S_6 are on and $S_4, S_5,$ and S_3 are off	1	v_i	0	$-v_i$
$S_2, S_3,$ and S_1 are on and $S_5, S_6,$ and S_4 are off	2	0	v_i	$-v_i$
$S_3, S_4,$ and S_3 are on and $S_6, S_7,$ and S_5 are off	3	$-v_i$	v_i	0
$S_4, S_5,$ and S_3 are on and $S_2, S_3,$ and S_1 are off	4	$-v_i$	0	v_i
$S_5, S_6,$ and S_4 are on and $S_3, S_4,$ and S_2 are off	5	0	$-v_i$	v_i
$S_6, S_1,$ and S_5 are on and $S_3, S_4,$ and S_2 are off	6	v_i	$-v_i$	0
$S_1, S_3,$ and S_5 are on and $S_4, S_6,$ and S_2 are off	7	0	0	0
$S_4, S_6,$ and S_2 are on and $S_1, S_3,$ and S_5 are off	8	0	0	0

Sinusoidal PWM technique:

In this case and in order to produce 120° out-of-phase load voltages, three modulating signals that are 120° out of phase are used. Figure 3.16 shows the ideal waveforms of three-phase VSI SPWM. In order to use a single carrier signal and preserve the features of the PWM technique, the normalized carrier frequency m_f should be an odd multiple of 3. Thus, all phase voltages (v_{aN} , v_{bN} , and v_{cN}) are identical, but 120° out-of-phase without even harmonics; moreover, harmonics at frequencies, a multiple of 3, are identical in amplitude and phase in all phases.

Therefore, for odd multiple of 3 values of the normalized carrier frequency m_f , the harmonics in the ac output voltage appear at normalized frequencies f_h centred around m_f and its multiples, specifically, at

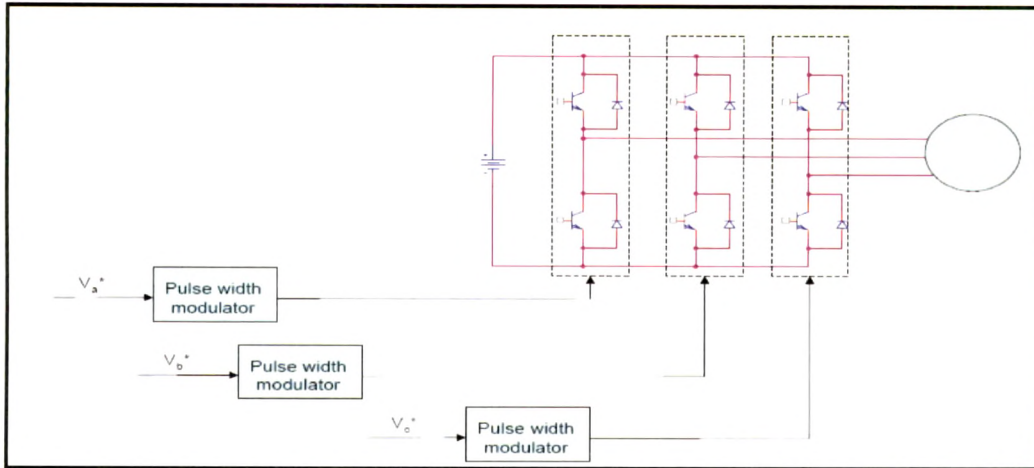


Fig 3.15 Block Diagram of three-phase inverter with SPWM technique

$$h = l_{mf} \pm k; \quad l = 1, 2, \dots$$

where $l = 1, 3, 5, \dots$ for $k = 2, 4, 6, \dots$ and $l = 2, 4, \dots$ for $k = 1, 5, 7, \dots$
 . such that h is not a multiple of 3.

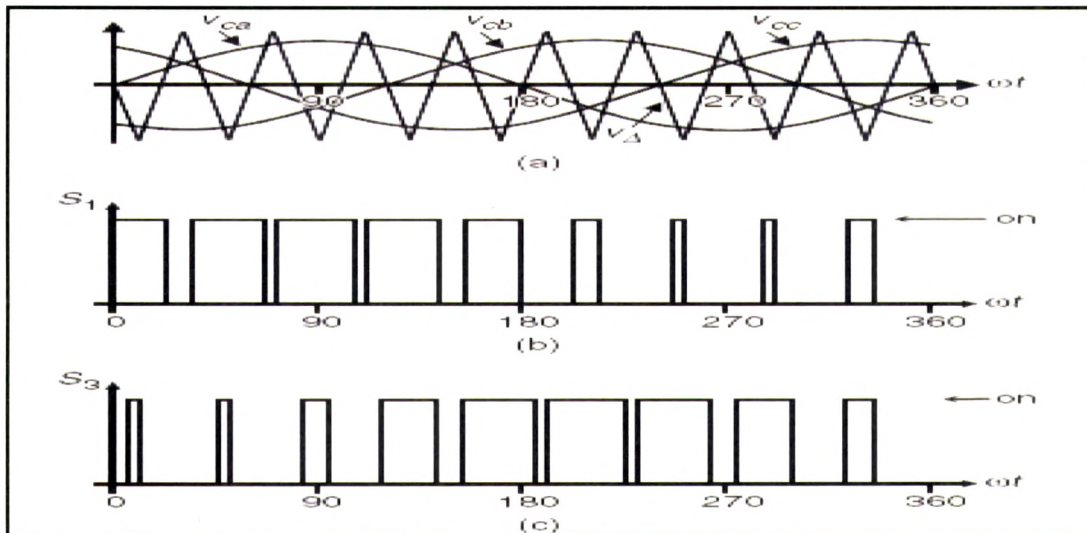


Fig 3.16 Principle of pulse generation using SPWM technique

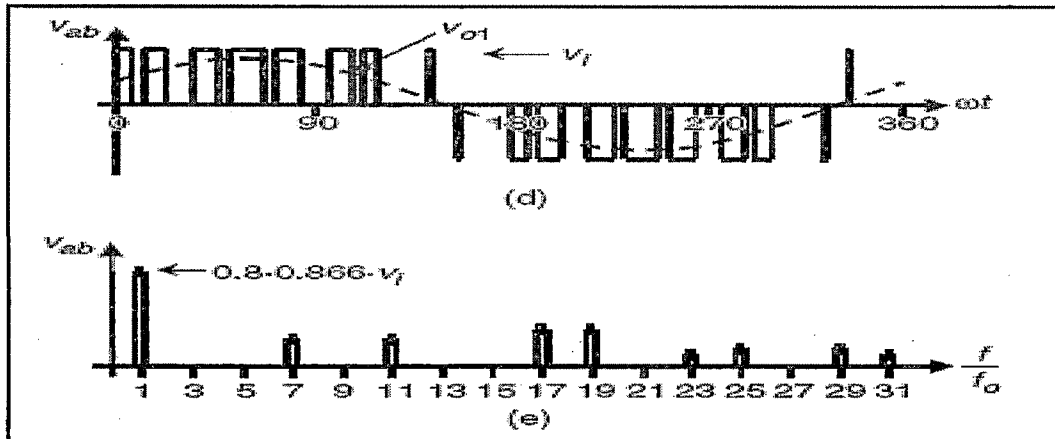


Fig 3.17 Inverter reference signal; output voltage V_{ab} ; harmonic spectrum of V_{ab}

Therefore, the harmonics will be at $mf \pm 2, mf \pm 4, \dots, 2mf \pm 1, 2mf \pm 5, \dots, 3mf \pm 2, 3mf \pm 4, \dots, 4mf \pm 1, 4mf \pm 5, \dots$. For nearly sinusoidal ac load current, the harmonics in the dc link current are at frequencies given by

$$h = l \cdot mf \pm k \quad l = 1, 2, \dots$$

where $l = 0, 2, 4, \dots$ for $k = 1, 5, 7, \dots$ and $l = 1, 3, 5, \dots$ for $k = 2, 4, 6, \dots$ such that $h = l \cdot mf \pm k$ is positive and not a multiple of 3.

The maximum amplitude of the fundamental phase voltage in the linear region of control ($m_a \leq 1$) is $v_i / 2$ and therefore the maximum amplitude of the fundamental ac output line to line voltage is $\sqrt{3} v_i / 2$. Therefore, one can write

$$\overset{\Delta}{v_{abl}} = m_a \cdot \sqrt{3} \cdot v_i / 2 \quad ; \quad 0 < m_a \leq 1 \quad (3.11)$$

Where m_a is the modulation index

To further increase the amplitude of the load voltage, the amplitude of the modulating signal v_c can be made higher than the amplitude of the carrier signal v_s , which leads to over modulation. The relationship between the amplitude of the fundamental ac output line voltage and the dc link voltage becomes non-linear as in single-phase VSIs. Thus, in the over modulation region, the line voltages range is

$$\sqrt{3} \frac{v_i}{2} < \hat{v}_{ab1} = \hat{v}_{bc1} = \hat{v}_{ca1} < \frac{4}{\pi} \sqrt{3} \frac{v_i}{2} \quad (3.12)$$

Space Vector PWM

The circuit model of a typical three-phase voltage source PWM inverter is shown in Fig. 3.18. S1 to S6 are the six power switches that shape the output, which are controlled by the switching variables a, a', b, b', c and c'. When an upper transistor is switched on, i.e., when a, b or c is 1, the corresponding lower transistor is switched off, i.e., the corresponding a', b' or c' is 0. Therefore, the on and off states of the upper transistors S1, S3 and S5 can be used to determine the output voltage.

The relationship between the switching variable vector [a, b, c]^t and the line-to-line voltage vector [V_{ab}, V_{bc}, V_{ca}]^t is given by following equation-3.14.

$$\begin{bmatrix} V_{ab} \\ V_{bc} \\ V_{ca} \end{bmatrix} = V_{dc} \begin{bmatrix} 1 & -1 & 0 \\ 0 & 1 & -1 \\ -1 & 0 & 1 \end{bmatrix} \begin{bmatrix} a \\ b \\ c \end{bmatrix} \quad (3.13)$$

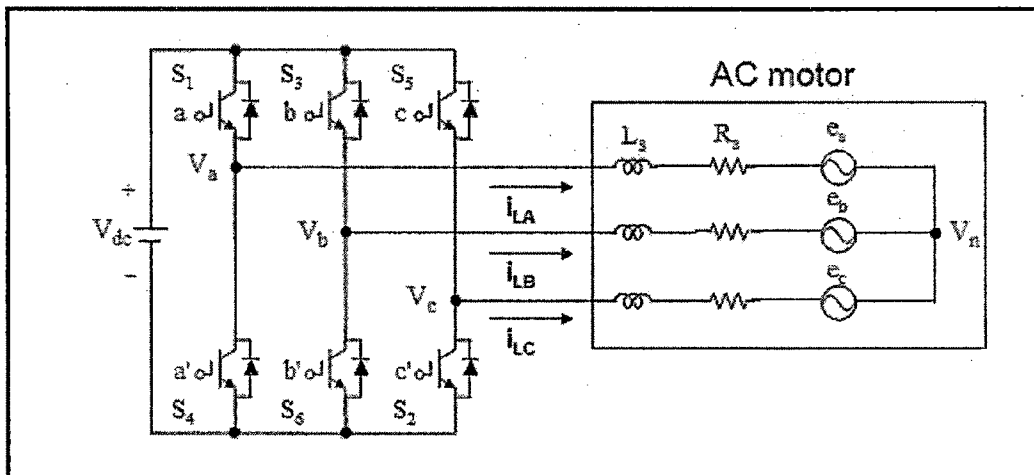


Fig 3.18 Three-phase inverter with R-L-E load

Also, the relationship between the switching variable vector [a, b, c]^t and the phase voltage vector [V_a, V_b, V_c]^t can be expressed as below.

$$\begin{bmatrix} V_{an} \\ V_{bn} \\ V_{cn} \end{bmatrix} = \frac{V_{dc}}{3} \begin{bmatrix} 2 & -1 & -1 \\ -1 & 2 & -1 \\ -1 & -1 & 2 \end{bmatrix} \begin{bmatrix} a \\ b \\ c \end{bmatrix} \quad (3.14)$$

As illustrated in Fig. 3.19, there are eight possible combinations of on and off patterns for the three upper power switches. The on and off states of the lower power devices are opposite to the upper one and so are easily determined once the states of the upper power transistors are determined. According to equations 3.14 and 3.15, the eight switching vectors, output line to neutral voltage (phase voltage), and output line-to-line voltages in terms of DC-link V_{dc} , are given in Table 3.3 and Fig. 3.19 shows the eight-inverter voltage vectors (V_0 to V_7).

Table 3.3 Voltage vectors, Switching vectors, Output phase voltages, Output line voltages

Voltage vectors	Switching vectors			Line to Neutral voltages			Line to line voltages		
	a	b	c	V_{an}	V_{bn}	V_{cn}	V_{ab}	V_{bc}	V_{ca}
V_0	0	0	0	0	0	0	0	0	0
V_1	1	0	0	$2/3$	$-1/3$	$-1/3$	1	0	-1
V_2	1	1	0	$1/3$	$1/3$	$-2/3$	0	1	-1
V_3	0	1	0	$-1/3$	$2/3$	$-1/3$	-1	1	0
V_4	0	1	1	$-2/3$	$1/3$	$1/3$	-1	0	1
V_5	0	0	1	$-1/3$	$-1/3$	$2/3$	0	-1	1
V_6	1	0	1	$1/3$	$-2/3$	$1/3$	1	-1	0
V_7	1	1	1	0	0	0	0	0	0

Note: Respective voltages should be multiplied by V_{dc} .

Space Vector PWM (SVPWM) refers to a special switching sequence of the upper three power transistors of a three-phase power inverter. It has been shown to generate less harmonic distortion in the output voltages and or currents applied to the phases of an AC motor and to provide

more efficient use of supply voltage compared with sinusoidal modulation technique.

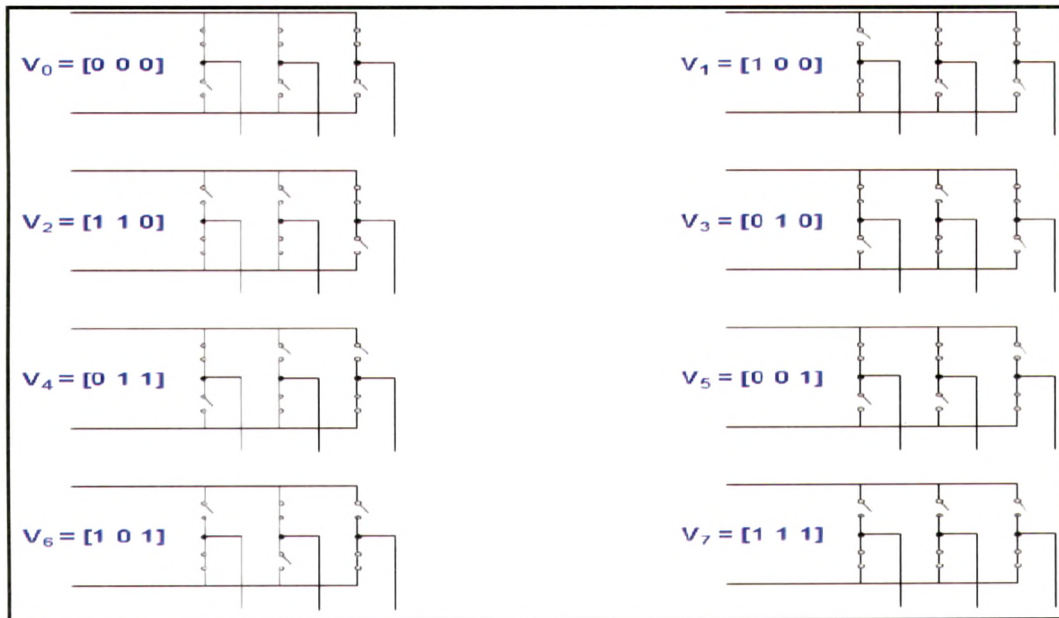


Fig. 3.19 Equivalent inverter circuit during various switching states

To implement the space vector PWM, the voltage equations in the abc reference frame can be transformed into the stationary dq reference frame that consists of the horizontal (d) and vertical (q) axes as depicted in Fig.3.20.

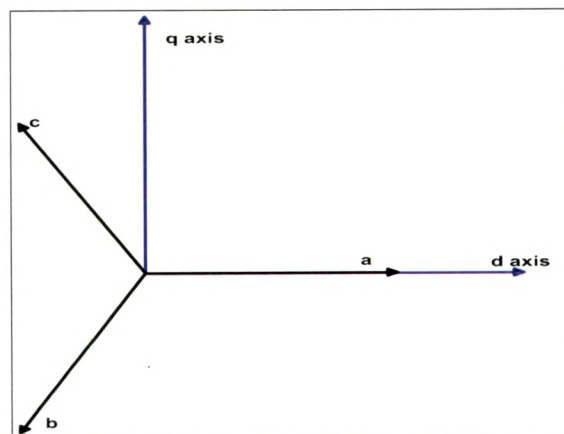


Fig. 3.20 The relationship of abc reference frame and stationary dq reference frame.

From this figure, the relation between these two reference frames is below

$$f_{dq0} = K_s f_{abc}$$

where $K_s = \sqrt{\frac{2}{3}} \begin{bmatrix} 1 & -\frac{1}{2} & -\frac{1}{2} \\ 0 & \frac{\sqrt{3}}{2} & -\frac{\sqrt{3}}{2} \\ \frac{1}{2} & \frac{1}{2} & \frac{1}{2} \end{bmatrix}$; $f_{dq0} = [f_d \ f_q \ f_0]^T$ & $f_{abc} = [f_a \ f_b \ f_c]^T$ and f

denotes either a voltage or a current variable.

As described in Fig. 3.19, this transformation is equivalent to an orthogonal projection of $[a, b, c]^t$ onto the two-axes perpendicular to the vector $[1, 1, 1]^t$ (the equivalent d-q plane) in a three-dimensional coordinate system. As a result, six non-zero vectors and two zero vectors are possible. Six nonzero vectors (V1 - V6) shape the axes of a hexagon as depicted in Fig. 3.21, and feed electric power to the load. The angle between any adjacent two non-zero vectors is 60 degrees. Meanwhile, two zero vectors (V0 and V7) are at the origin and apply zero voltage to the load. The eight vectors are called the basic space vectors and are denoted by V0, V1, V2, V3, V4, V5, V6, and V7. The same transformation can be applied to the desired output voltage to get the desired reference voltage vector Vref in the d-q plane.

The objective of space vector PWM technique is to approximate the reference voltage vector Vref using the eight switching patterns. One simple method of approximation is to generate the average output of the inverter in a small period, T to be the same as that of Vref in the same period (refer fig 3.21).

Therefore, space vector PWM can be implemented by the following steps:

- Step 1. Determine V_d , V_q , V_{ref} , and angle (α)
- Step 2. Determine time duration T_1 , T_2 , T_0

- Step 3. Determine the switching time of each transistor (S_1 to S_6)

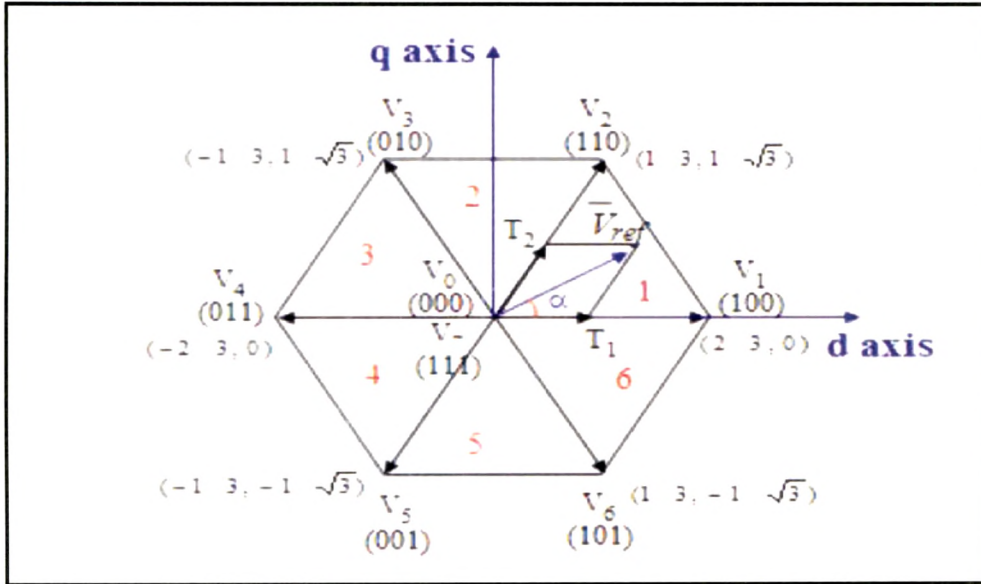


Fig. 3.21 Basic switching vectors and sectors.

Determination of V_d , V_q and the angle (α)

From the fig. 3.22, the value of V_d and V_q can be determined as follows

$$V_d = V_{an} - V_{bn} \cos 60^\circ - V_{cn} \cos 60^\circ$$

$$V_d = V_{an} - \frac{1}{2}V_{bn} - \frac{1}{2}V_{cn}$$

$$V_q = 0 - V_{bn} \cos 30^\circ + V_{cn} \cos 30^\circ$$

$$V_q = 0 - \frac{\sqrt{3}}{2}V_{bn} + \frac{\sqrt{3}}{2}V_{cn}$$

$$\begin{bmatrix} V_d \\ V_q \end{bmatrix} = \begin{bmatrix} 1 & -1/2 & -1/2 \\ 0 & \sqrt{3}/2 & -\sqrt{3}/2 \end{bmatrix} \begin{bmatrix} V_{an} \\ V_{bn} \\ V_{cn} \end{bmatrix}; |V_{ref}| = \sqrt{V_d^2 + V_q^2}$$

$$\alpha = \tan^{-1}\left(\frac{V_q}{V_d}\right) = \omega t = 2\pi f t; \text{ where } f \text{ is fundamental frequency}$$

Determine time duration T_1, T_2, T_0

From the figure 3.23, the switching duration can be calculated as follows:

If we consider for sector one

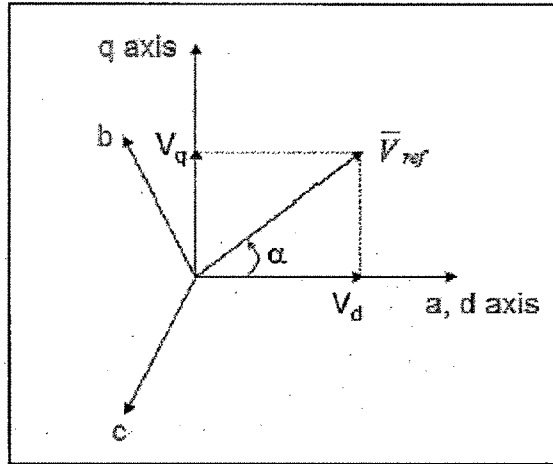


Fig. 3.22 Voltage Space Vector and its components in (d, q)

$$\int_0^{T_z} \bar{V}_{ref} dt = \int_0^{T_1} \bar{V}_1 dt + \int_{T_1}^{T_1+T_2} \bar{V}_2 dt + \int_{T_1+T_2}^{T_z} \bar{V}_0 dt$$

$$\therefore T_z * V_{ref} = (T_1 * \bar{V}_1 + T_2 * \bar{V}_2)$$

$$\Rightarrow T_z * |\bar{V}_{ref}| * \begin{bmatrix} \cos(\alpha) \\ \sin(\alpha) \end{bmatrix} = T_1 * \frac{2}{3} * V_{dc} * \begin{bmatrix} 1 \\ 0 \end{bmatrix} + T_2 * \frac{2}{3} * V_{dc} * \begin{bmatrix} \cos(\pi/3) \\ \sin(\pi/3) \end{bmatrix};$$

where $(0 \leq \alpha \leq 60^\circ)$

$$\begin{aligned} T_z * |\bar{V}_{ref}| * \cos(\alpha) &= T_1 * \frac{2}{3} * V_{dc} + T_2 * \frac{2}{3} * V_{dc} * \cos(\pi/3) \\ \therefore T_z * |\bar{V}_{ref}| * \sin(\alpha) &= T_1 * 0 + T_2 * \frac{2}{3} * V_{dc} * \sin(\pi/3) \\ \therefore T_z * |\bar{V}_{ref}| * \sin(\alpha) &= T_2 * \frac{2}{3} * V_{dc} * \sin(\pi/3) \\ \therefore T_2 &= \frac{T_z * |\bar{V}_{ref}| * \sin(\alpha)}{\frac{2}{3} * V_{dc} * \sin(\pi/3)} \end{aligned}$$

Substituting the value of T_2 from the last equation of above block in first equation

$$\begin{aligned}
 T_z * |\bar{V}_{ref}| * \cos(\alpha) &= T_1 * \frac{2}{3} * V_{dc} + \frac{T_z * |\bar{V}_{ref}| * \sin(\alpha) * \frac{2}{3} * V_{dc} * \cos(\pi/3)}{\frac{2}{3} * V_{dc} * \sin(\pi/3)} \\
 \therefore T_z * |\bar{V}_{ref}| * \sin(\pi/3) * \cos(\alpha) &= T_1 * \frac{2}{3} * V_{dc} * \sin(\pi/3) + T_z * |\bar{V}_{ref}| * \sin(\alpha) * \cos(\pi/3) \\
 \therefore T_1 &= \frac{T_z * |\bar{V}_{ref}| * (\sin(\pi/3) * \cos(\alpha) - \sin(\alpha) * \cos(\pi/3))}{\frac{2}{3} * V_{dc} * \sin(\pi/3)} \\
 \therefore T_1 &= \frac{T_z * |\bar{V}_{ref}| * (\sin(\pi/3 - \alpha))}{\frac{2}{3} * V_{dc} * \sin(\pi/3)}
 \end{aligned}$$

$$\therefore T_0 = T_z - (T_1 - T_2) \quad \text{where, } T_z = \frac{1}{f_z}$$

In general for any sector the values of T_1 , T_2 and T_0 can be determined by following equations

$$\begin{aligned}
 \therefore T_1 &= \frac{\sqrt{3} * T_z * |\bar{V}_{ref}|}{V_{dc}} * \left(\sin\left(\pi/3 - \alpha + \frac{n-1}{3}\pi\right) \right) \\
 &= \frac{\sqrt{3} * T_z * |\bar{V}_{ref}|}{V_{dc}} * \left(\sin\frac{n}{3}\pi - \alpha \right) \\
 &= \frac{\sqrt{3} * T_z * |\bar{V}_{ref}|}{V_{dc}} * \left(\sin\frac{n}{3}\pi \cos\alpha - \cos\frac{n}{3}\pi \sin\alpha \right) \\
 \therefore T_2 &= \frac{\sqrt{3} * T_z * |\bar{V}_{ref}|}{V_{dc}} * \left(\sin\left(\alpha - \frac{n-1}{3}\pi\right) \right) \\
 &= \frac{\sqrt{3} * T_z * |\bar{V}_{ref}|}{V_{dc}} * \left(-\cos\alpha \sin\frac{n-1}{3}\pi + \cos\frac{n-1}{3}\pi \sin\alpha \right)
 \end{aligned}$$

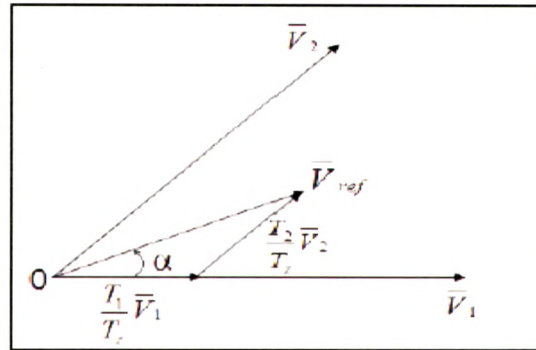
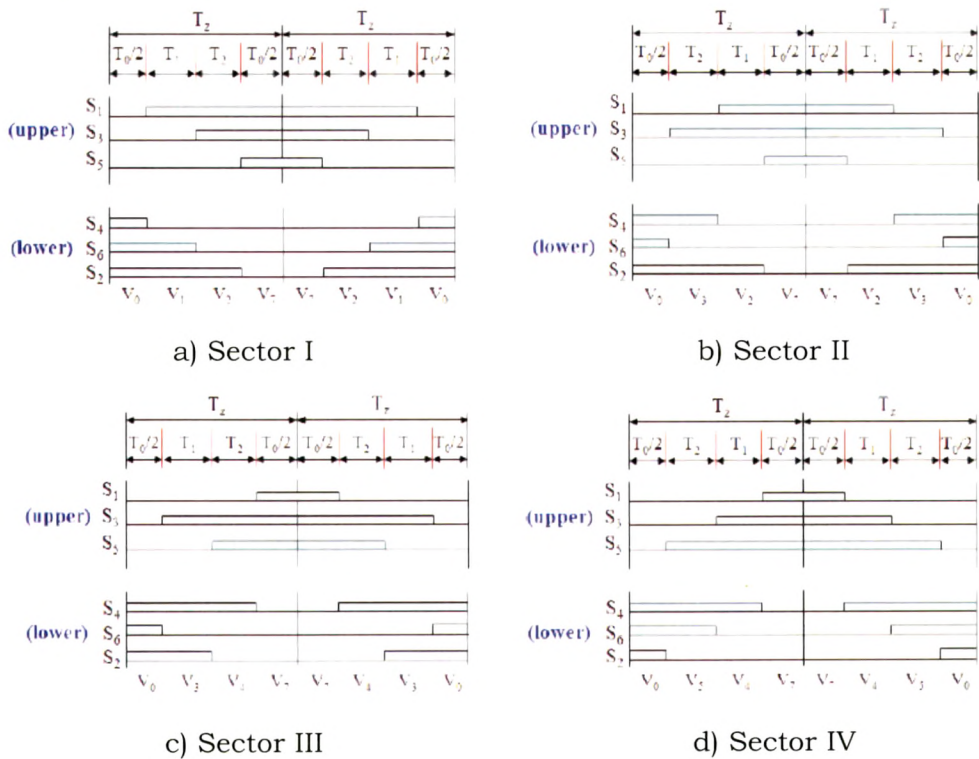


Fig 3.23 Reference vector as a combination of adjacent vectors at sector 1.

After determination of sector and the time duration of application of each vector i.e. T_1 , T_2 & T_0 ; now it is important to implement the SVPWM technique by appropriate allocation of switching vectors. Space vector switching pattern at each sector is shown in figure 3.24 below. Further the switching time at each vector can be summarized in the following table based on fig. 3.24



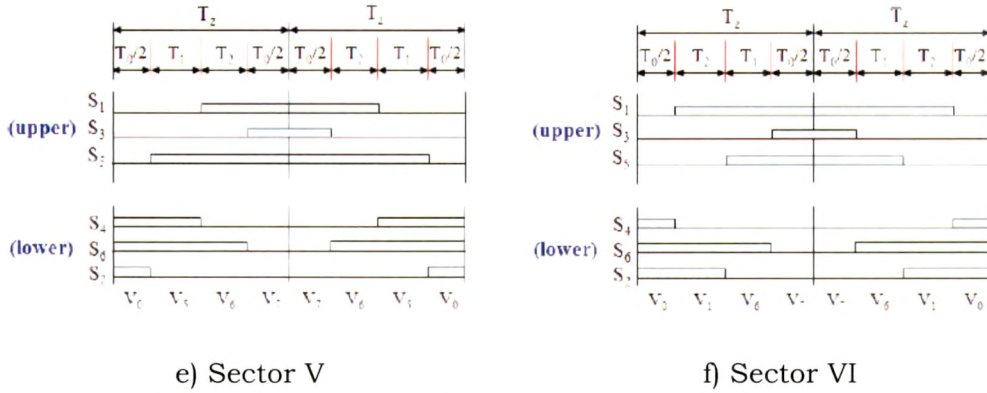


Fig 3.24 Space Vector PWM switching patterns at each sector

Table 3.4: Switching Time Calculation at Each Sector

Sector No	Upper Switches (S ₁ , S ₃ , S ₅)	Lower Switches (S ₄ , S ₆ , S ₂)
I	$S_1 = T_1 + T_2 + \frac{T_0}{2}$ $S_3 = T_2 + \frac{T_0}{2}$ $S_5 = \frac{T_0}{2}$	$S_4 = \frac{T_0}{2}$ $S_6 = T_1 + \frac{T_0}{2}$ $S_2 = T_1 + T_2 + \frac{T_0}{2}$
II	$S_1 = T_1 + \frac{T_0}{2}$ $S_3 = T_1 + T_2 + \frac{T_0}{2}$ $S_5 = \frac{T_0}{2}$	$S_4 = T_2 + \frac{T_0}{2}$ $S_6 = \frac{T_0}{2}$ $S_2 = T_1 + T_2 + \frac{T_0}{2}$
III	$S_1 = \frac{T_0}{2}$ $S_3 = T_1 + T_2 + \frac{T_0}{2}$ $S_5 = T_2 + \frac{T_0}{2}$	$S_4 = T_1 + T_2 + \frac{T_0}{2}$ $S_6 = \frac{T_0}{2}$ $S_2 = T_1 + \frac{T_0}{2}$
IV	$S_1 = \frac{T_0}{2}$ $S_3 = T_1 + \frac{T_0}{2}$ $S_5 = T_1 + T_2 + \frac{T_0}{2}$	$S_4 = T_1 + T_2 + \frac{T_0}{2}$ $S_6 = T_2 + \frac{T_0}{2}$ $S_2 = \frac{T_0}{2}$

V	$S_1 = T_2 + \frac{T_0}{2}$ $S_3 = \frac{T_0}{2}$ $S_5 = T_1 + T_2 + \frac{T_0}{2}$	$S_4 = T_1 + \frac{T_0}{2}$ $S_6 = T_1 + T_2 + \frac{T_0}{2}$ $S_2 = \frac{T_0}{2}$
VI	$S_1 = T_1 + T_2 + \frac{T_0}{2}$ $S_3 = \frac{T_0}{2}$ $S_5 = T_1 + \frac{T_0}{2}$	$S_4 = \frac{T_0}{2}$ $S_6 = T_1 + T_2 + \frac{T_0}{2}$ $S_2 = T_2 + \frac{T_0}{2}$

For the sake of simplicity and decrease the computation time, SPWM technique is used for generation of variable frequency voltages across the load.

3.5 Simulation of the Proposed Technique:

The proposed topology employing the high frequency link is simulated using MATLAB Simulink software. The results illustrate the advantages of the proposed topology. Simulation is carried out considering following parameters as input reference.

System parameters:

Case I

Input voltage: 415 Volts, 3-phase

Input frequency: 50 Hz

Output voltage: User selectable (0-400 volts range), three phase

Output frequency: user selectable, (30 Hz is set)

Output load parameters: $R = 10$ ohms, $L = 19$ mH

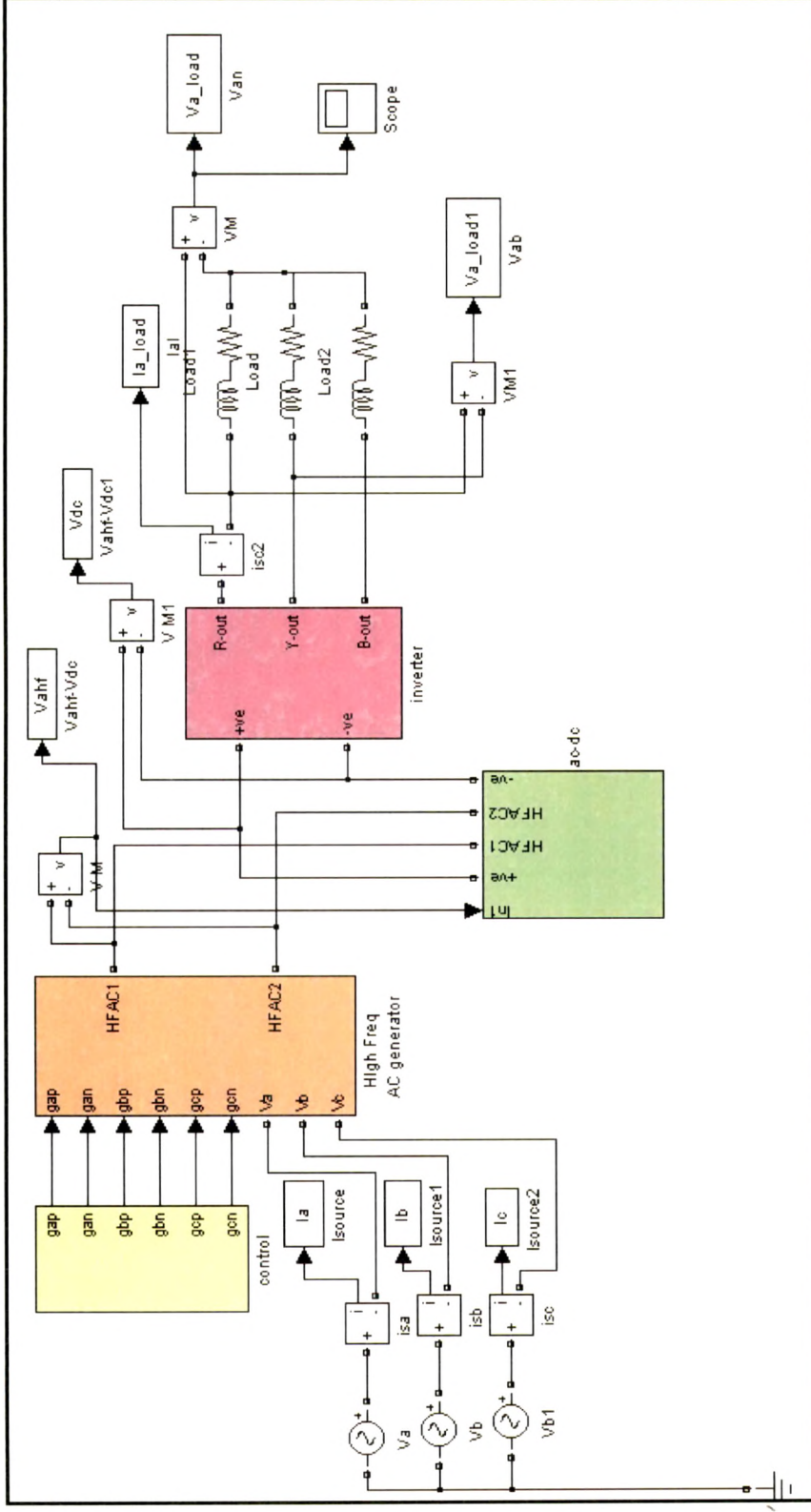


Fig.S_{3.5} Simulation block diagram for complete Direct AC-AC converter

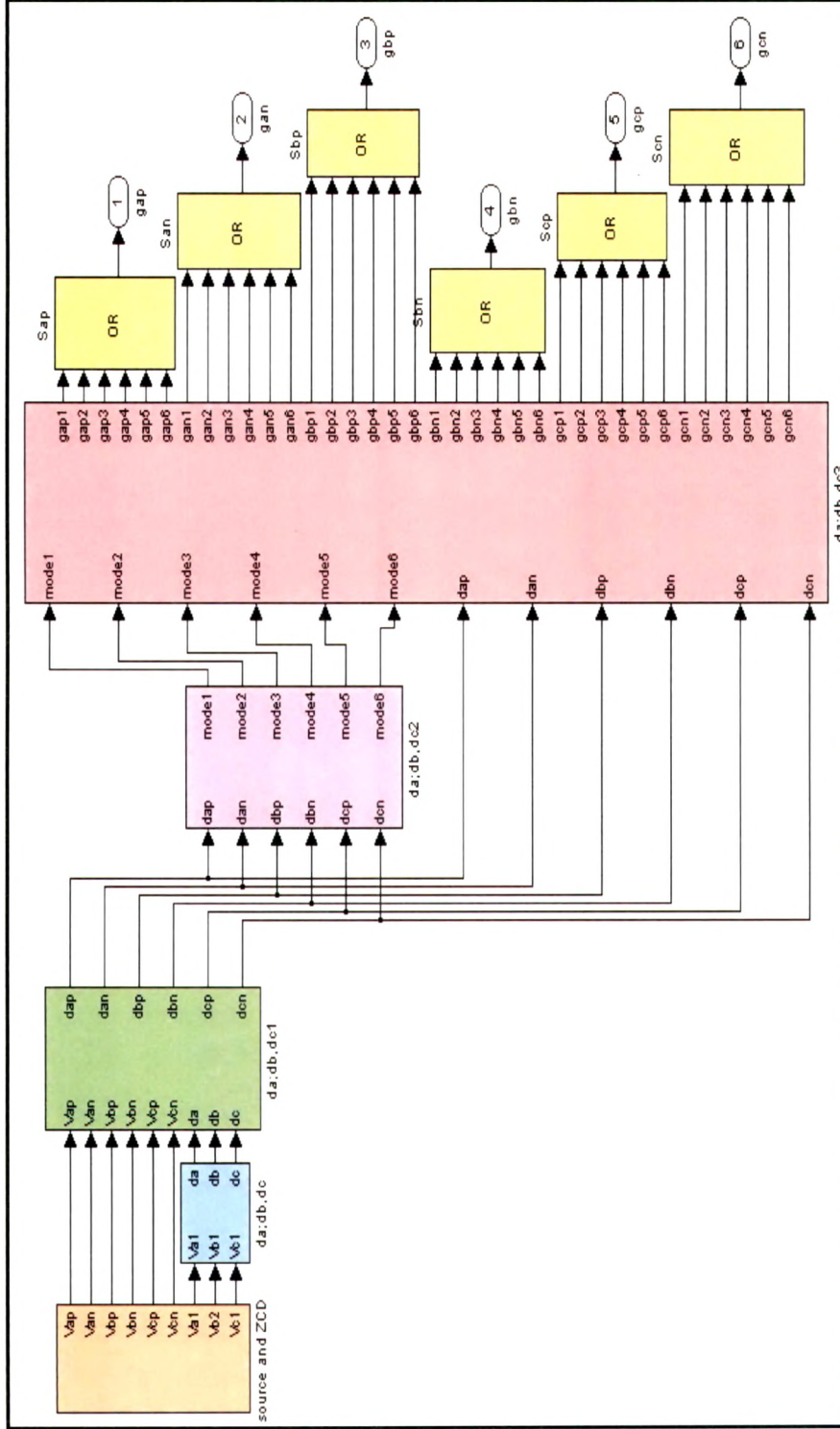


Fig.S.3.6 Control circuit block diagram for 3-phase to 1-phase conversion

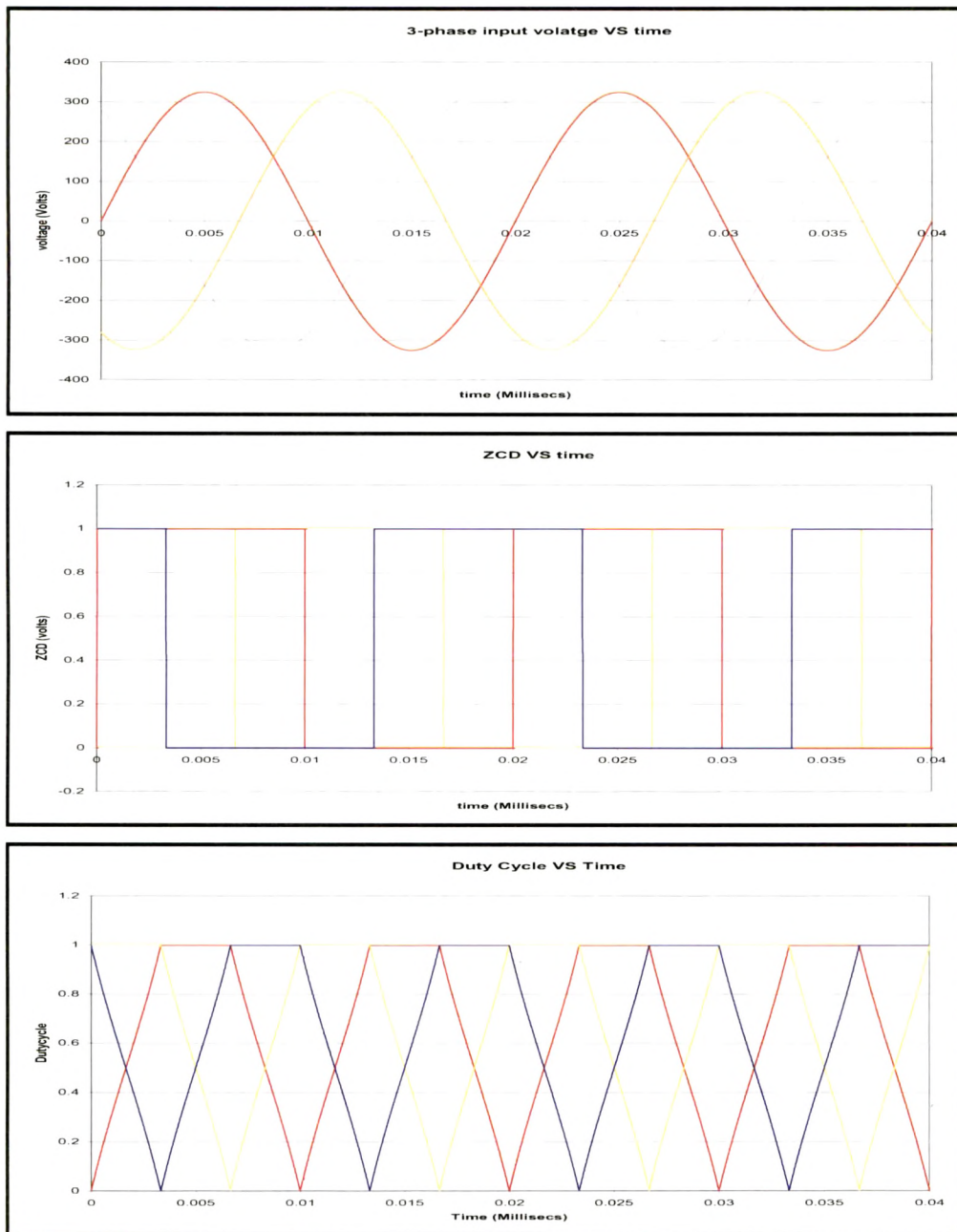


Fig.S3.7 a. Three phase source voltages

b. Waveforms showing zero crossing for three phase source voltages

c. Duty cycle calculation for all three phases

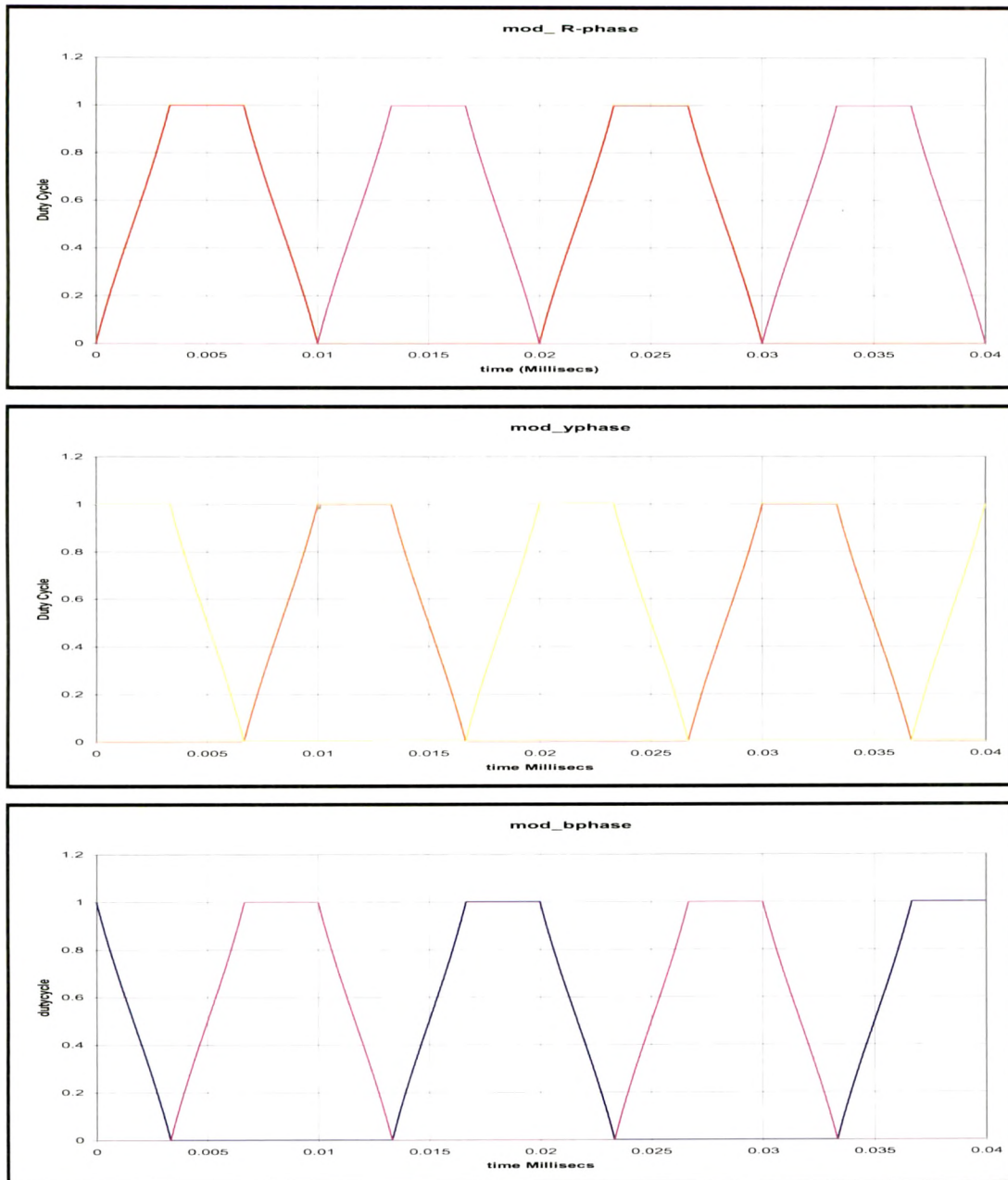


Fig.S3.8. **a. Duty cycle calculation waveforms for R-phase**
 b. Duty cycle calculation waveforms for Y-phase
 c. Duty cycle calculation waveforms for B-phase

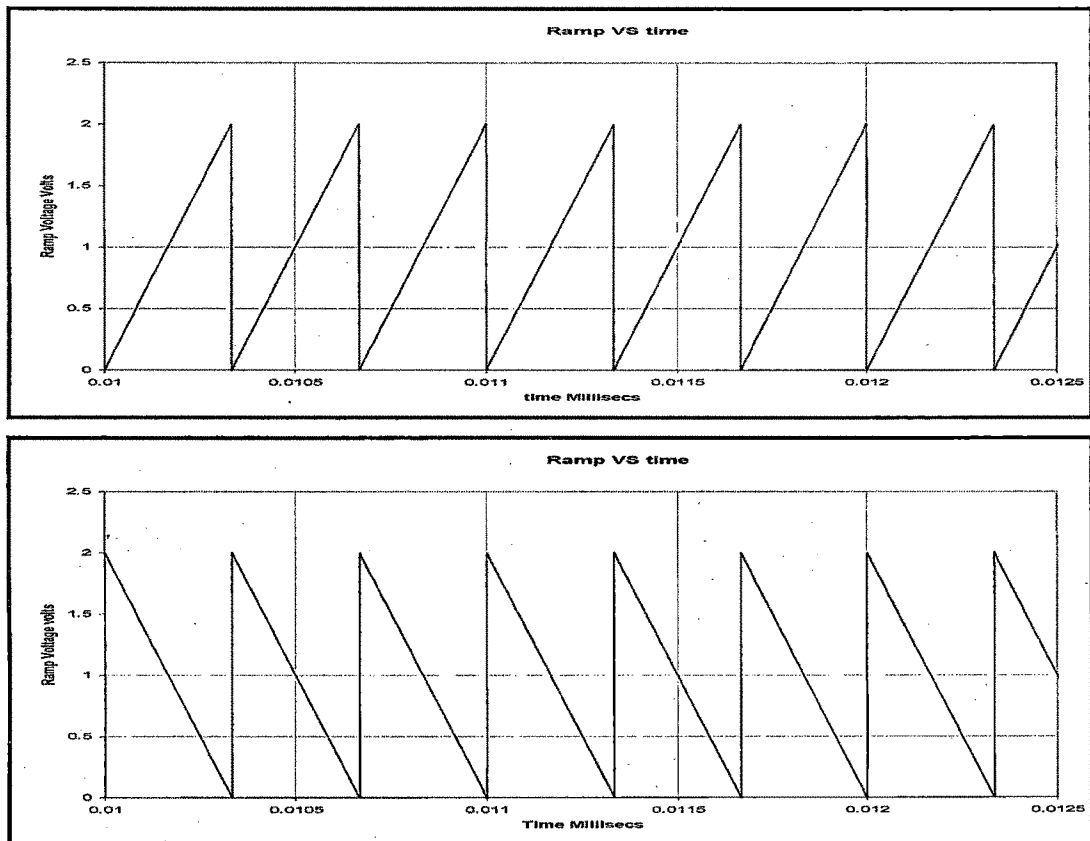


Fig.S3.9. a. Positive ramp signals as carriers for modulation
 b. Negative ramp signals as carriers for modulation

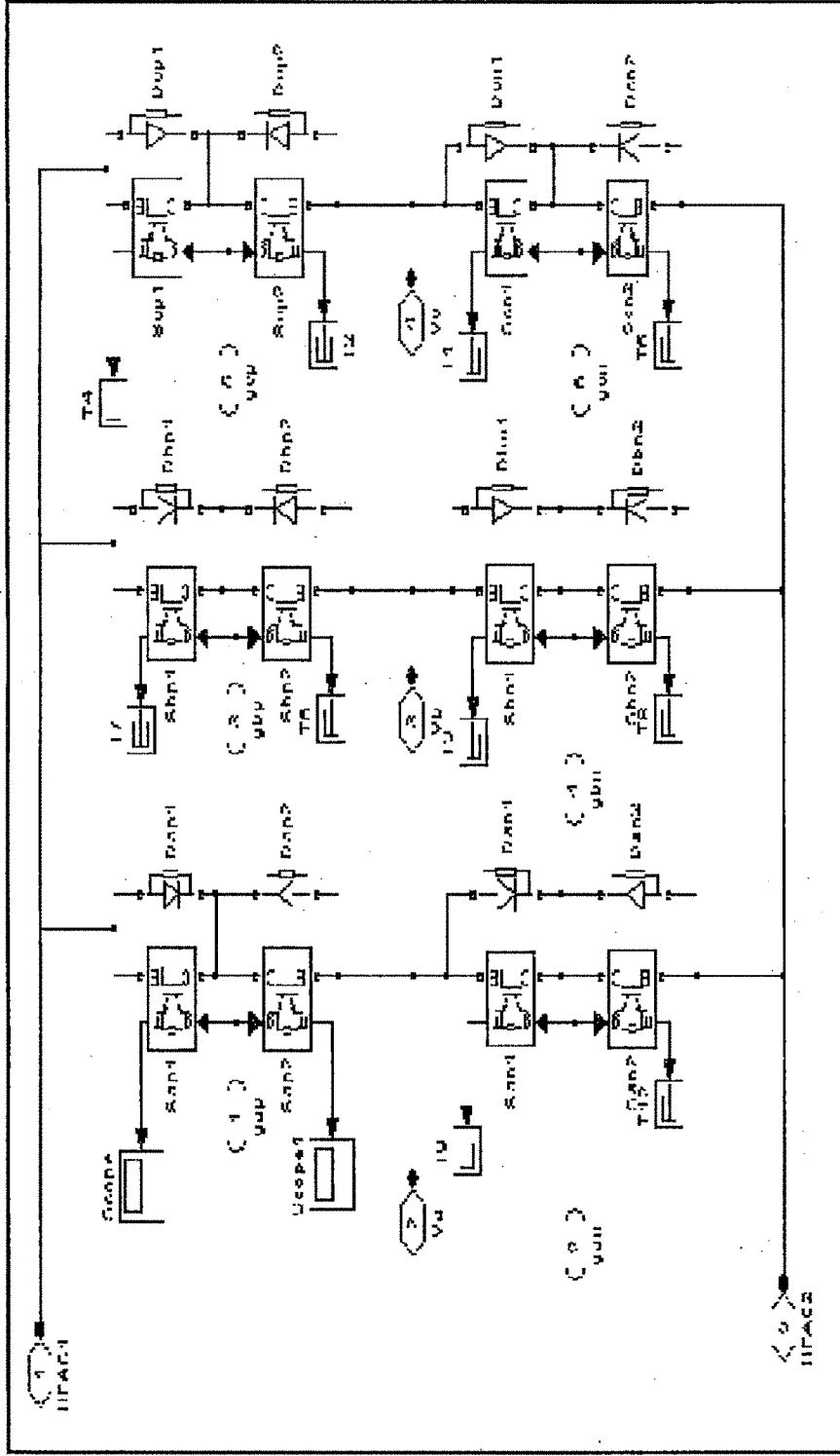


Fig.S3.10 Power circuit of primary converter implemented using bidirectional switches considering all the parameters as in real case

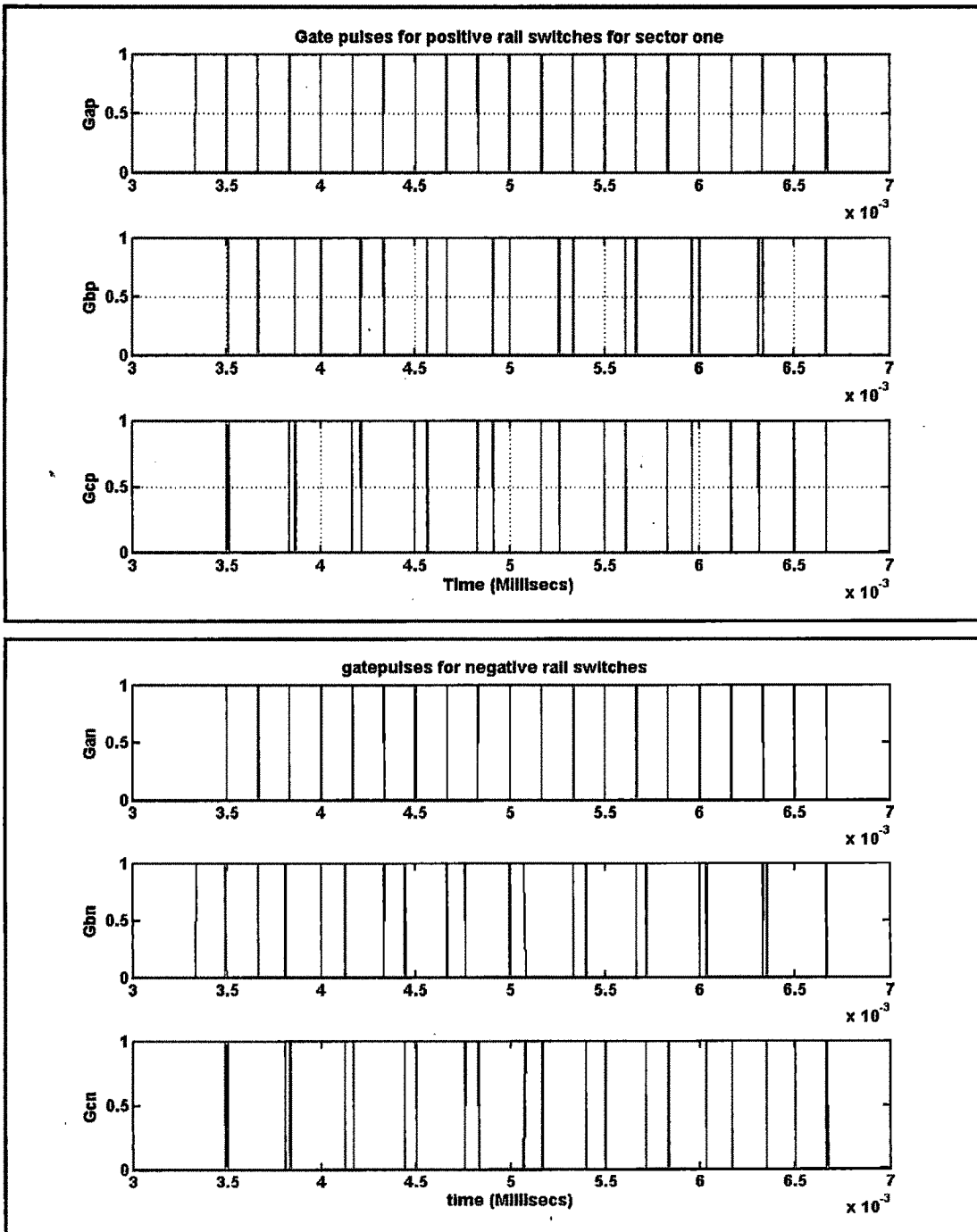


Fig.S_{3.11} a. Gate pulses for R-phase positive rail switches
 b. Gate pulses for R-phase negative rail switches

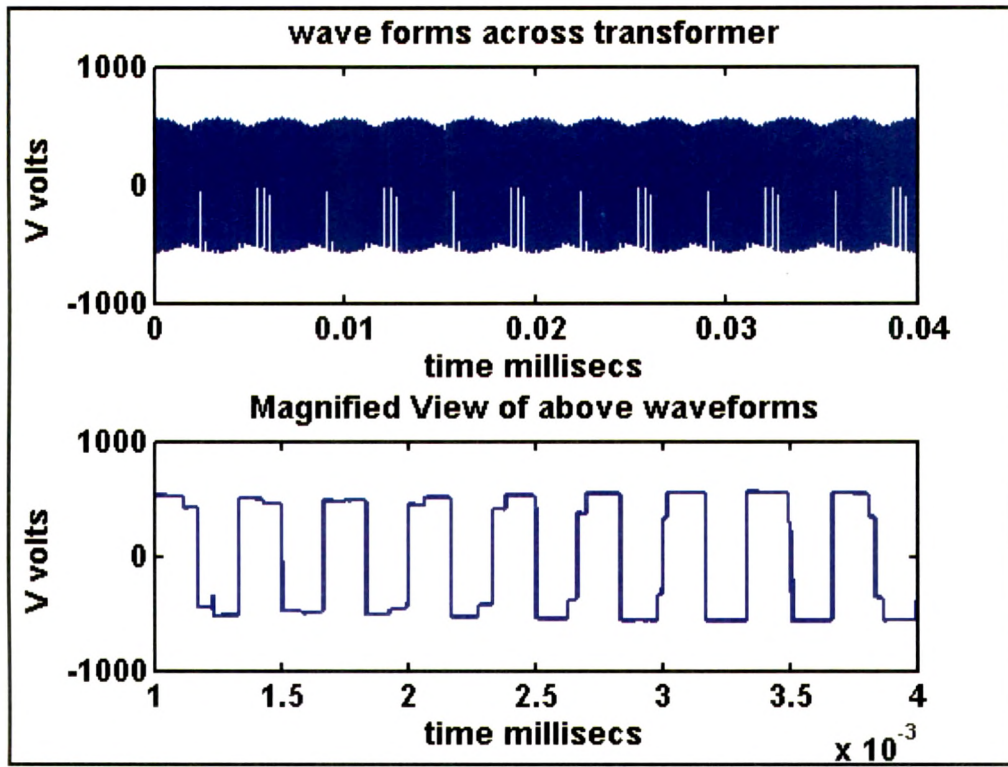


Fig.S3.12 Voltage waveforms across High frequency transformer and its magnified view.

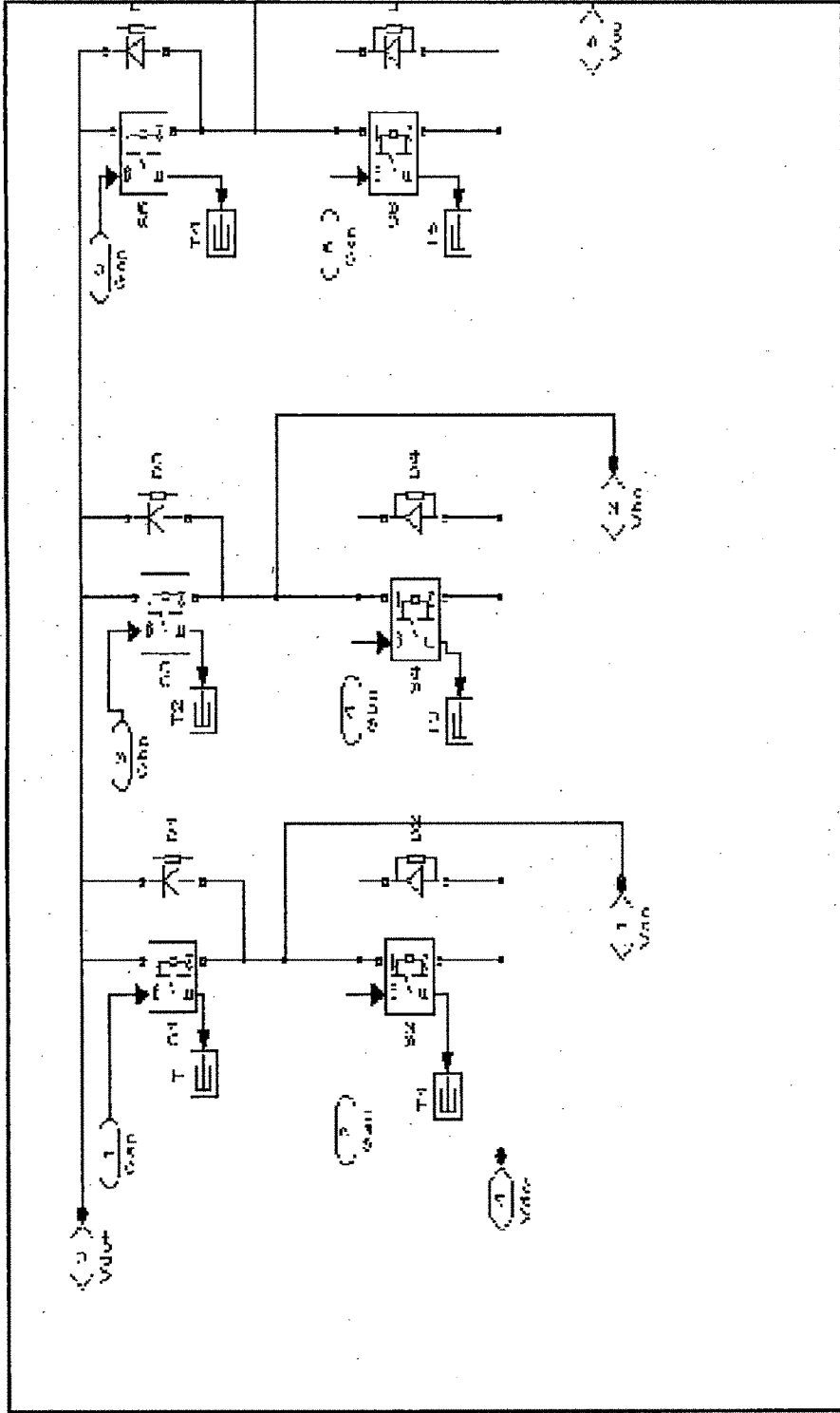


Fig.S3.13 Secondary converter implemented using IGBTs and Diodes

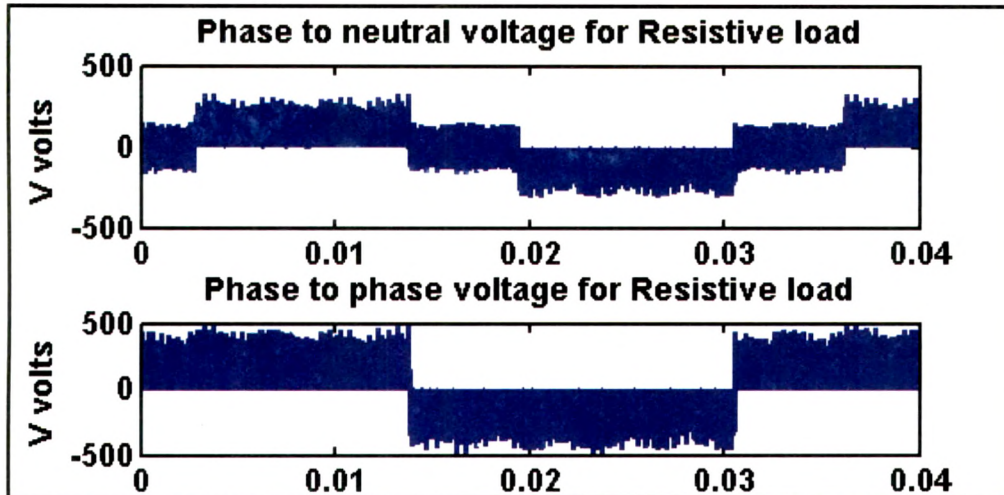


Fig.S3.14 Voltage waveforms across Resistive load

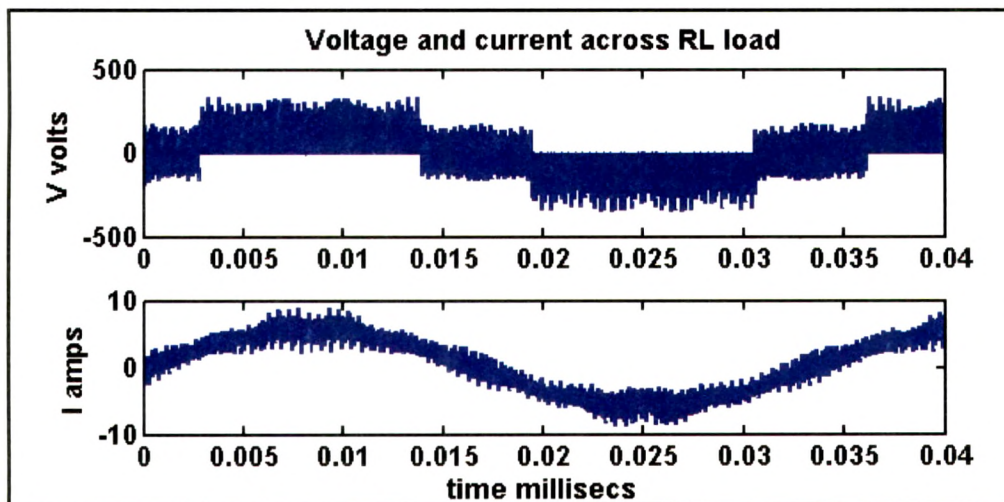


Fig.S3.15 Voltage and current waveform across Inductive load

3.5 Conclusion

The control algorithm for the generalized configuration explained in chapter 2 is complex and difficult to implement. In this chapter a new configuration is proposed with simple and robust control technique wherein the output voltage magnitude is independent of the input voltages and is fully controllable. Detailed simulations have been carried out and the results validate the model proposed.